Proton Form Factors: Recent Developments

Andrew Puckett
Los Alamos National Laboratory
University of Virginia Nuclear Physics Seminar
11/23/2010

Jefferson Lab

Experimental Hall C

Outline

- Introduction
- Nucleon form factors overview
- Experiments E04-108 and E04-019 overview
- Data analysis
- Results
  - **E04-108 final results (published in PRL)**
  - **E04-019 preliminary results (to be submitted to PRL)**
  - **E99-007 reanalysis**
- Theoretical overview
  - Nucleon Form Factors
  - TPEX in elastic ep scattering
- Statistical Impact of E04-108 results
- Conclusion/Outlook

Introduction

- Unlike the electron, the proton is not a pointlike, elementary particle
- A proton is a complicated object with internal structure and an extended distribution of charge and current
- Naively, a proton is a bound state of three spin-1/2 ***quarks***, held together by strongly attractive ***color*** forces mediated by ***gluons.***
- Quarks are light; mass = few MeV, while proton mass ~1 GeV→Enormous ratio of binding energy/constituent mass; bound in the proton move relativistically
- $E=mc^2$; creation and annihilation of quarks and antiquarks in the proton; "dresses" constituent quarks in a "sea" of quark-antiquark pairs and gluons.
- Quarks also carry ***electric*** charge; physicists can precisely probe the quarks deep inside the proton using high-energy electron beams which interact with quarks through the well-known electromagnetic force.
- The goal of precision experimental studies of the quark structure of the proton is to understand how the static properties and dynamical behavior of protons and neutrons (nucleons) emerge from QCD, the theory of the elementary strong interactions between quarks

Overview of Nucleon Form Factors

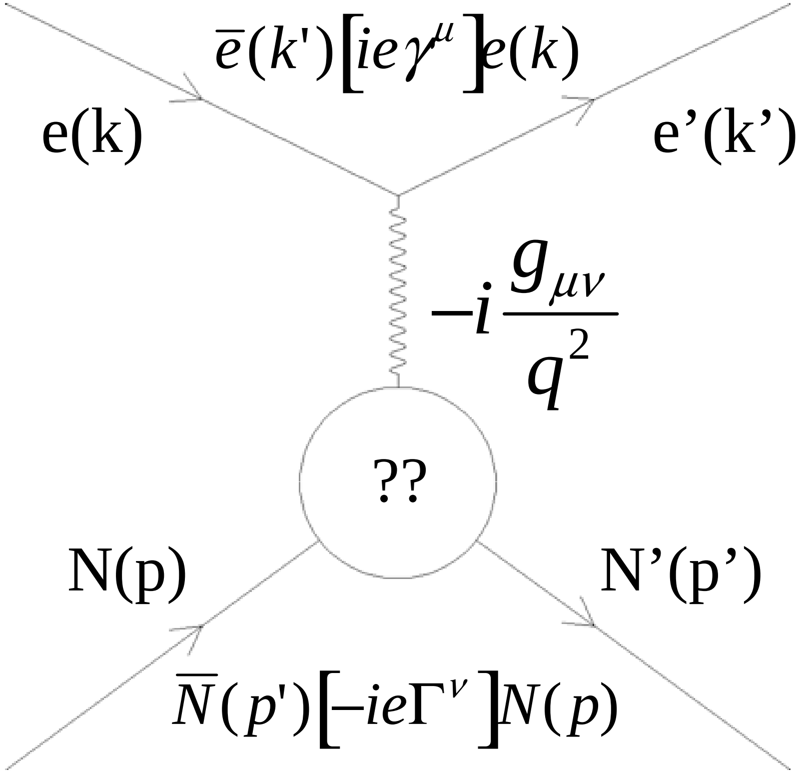

One-photon exchange (OPEX) mechanism for elastic *eN* scattering

Definitions and Formulas:

$$\Gamma^{\mu} = F_1(q^2)\gamma^{\mu} + F_2(q^2)\frac{i\sigma^{\mu\nu}q_{\nu}}{2M}$$

$$Q^2 = -q^2 > 0$$

$$G_E = F_1 - \tau F_2$$

$$G_M = F_1 + F_2$$

$$\tau \equiv \frac{Q^2}{4M^2}$$

$$\frac{d\sigma}{d\Omega_e} = \frac{\alpha^2}{Q^2}\left(\frac{E_e^{'}}{E_e}\right)\left[\frac{G_E^2 + \tau G_M^2}{1+\tau}\cot^2\left(\frac{\theta_e}{2}\right) + 2\tau G_M^2\right]$$

Lab Differential Cross Section: Rosenbluth Formula

Rosenbluth (L/T) Separation

$$\sigma_r \equiv (1+\tau)\varepsilon \frac{\sigma_{eN}}{\sigma_{Mott}} = \varepsilon G_E^2 + \tau G_M^2$$

$$\varepsilon = \left[1 + 2(1+\tau)\tan^2\left(\frac{\theta_e}{2}\right)\right]^{-1}$$

- Measure angular dependence of scattering cross section at fixed Q^2
- In OPEX, "reduced cross section" is linear in ε
- Slope and intercept determine G_E^2, G_M^2 respectively

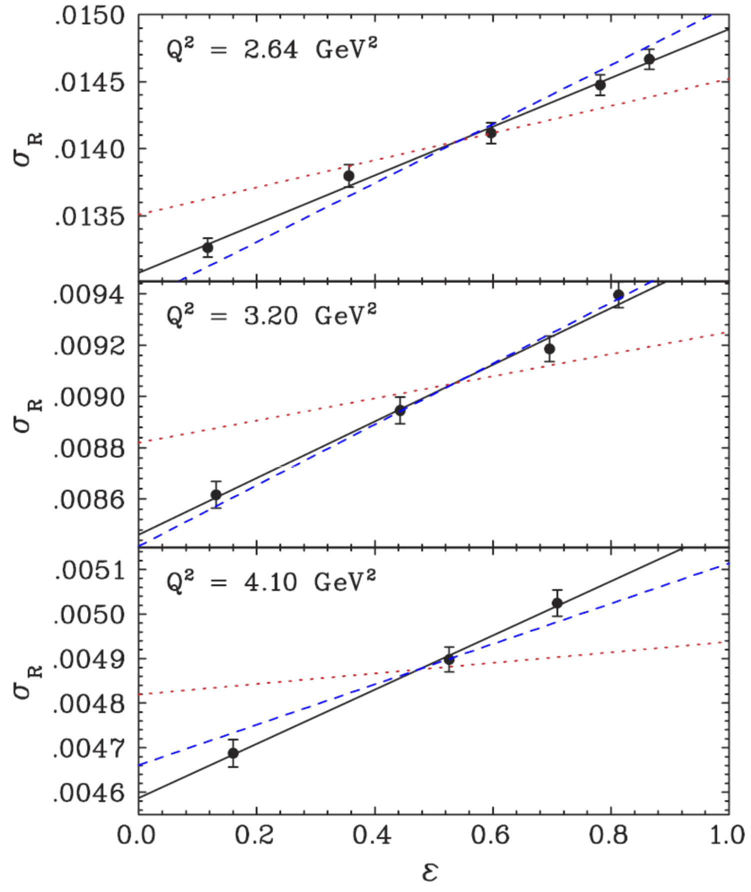

PRL 94, 142301 (2005)

World Cross-Section Data

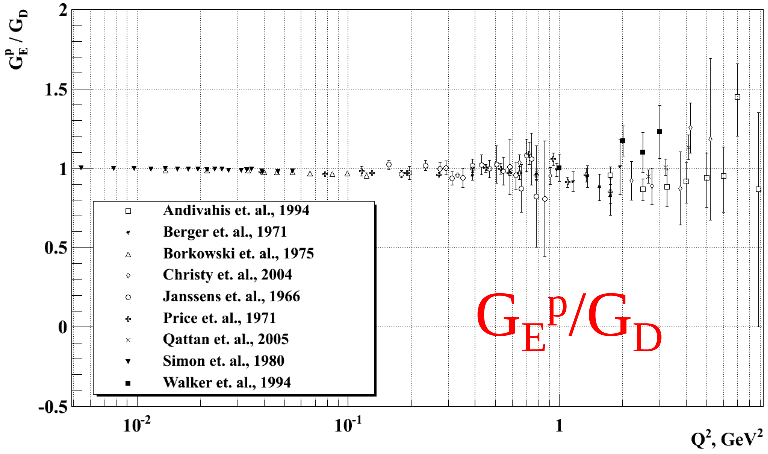

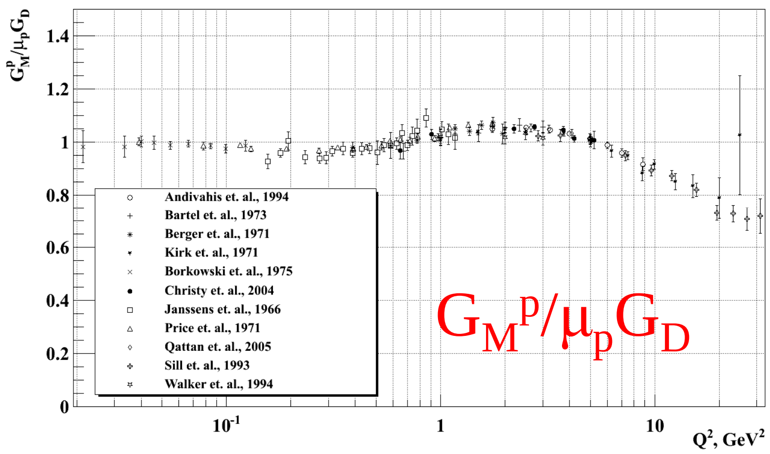

- Cross section data for G_E^p, G_M^p, G_M^n qualitatively described by dipole form:

$$G_D = \left(1 + \frac{Q^2}{\Lambda^2}\right)^{-2} \qquad \Lambda^2 = 0.71\ \mathrm{GeV}^2$$

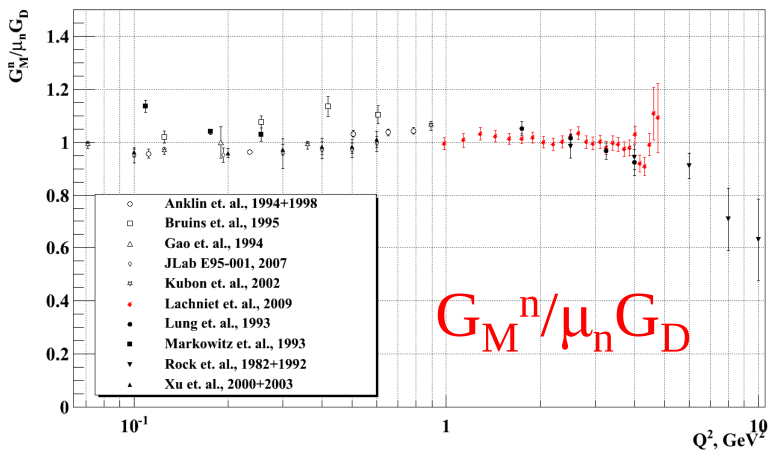

- L/T separation becomes insensitive to $G_M(G_E)$ at small (large) Q^2
- Method impractical for (small) G_E^n

Polarization Transfer

$$p(\vec{e},e'\vec{p})$$

$$I_0 P_l = \sqrt{\tau(1+\tau)}\tan^2\left(\frac{\theta_e}{2}\right)\frac{E_e + E_e^{'}}{M}G_M^2$$

$$I_0 P_t = -2\sqrt{\tau(1+\tau)}\tan\left(\frac{\theta_e}{2}\right)G_E G_M$$

$$P_n = 0$$

$$I_0 \equiv G_E^2 + \frac{\tau}{\varepsilon}G_M^2$$

$$\frac{G_E}{G_M} = -\frac{P_t}{P_l}\frac{E_e + E_e^{'}}{2M}\tan\left(\frac{\theta_e}{2}\right)$$

- Elastic scattering of polarized electrons from unpolarized nucleons transfers polarization to scattered nucleons
- Better sensitivity to G_E, especially at high Q^2
- Determines sign of G_E/G_M
- Much lower sensitivity to radiative corrections and two-photon-exchange (TPEX) than Rosenbluth

Polarization Transfer and G_E^p/G_M^p

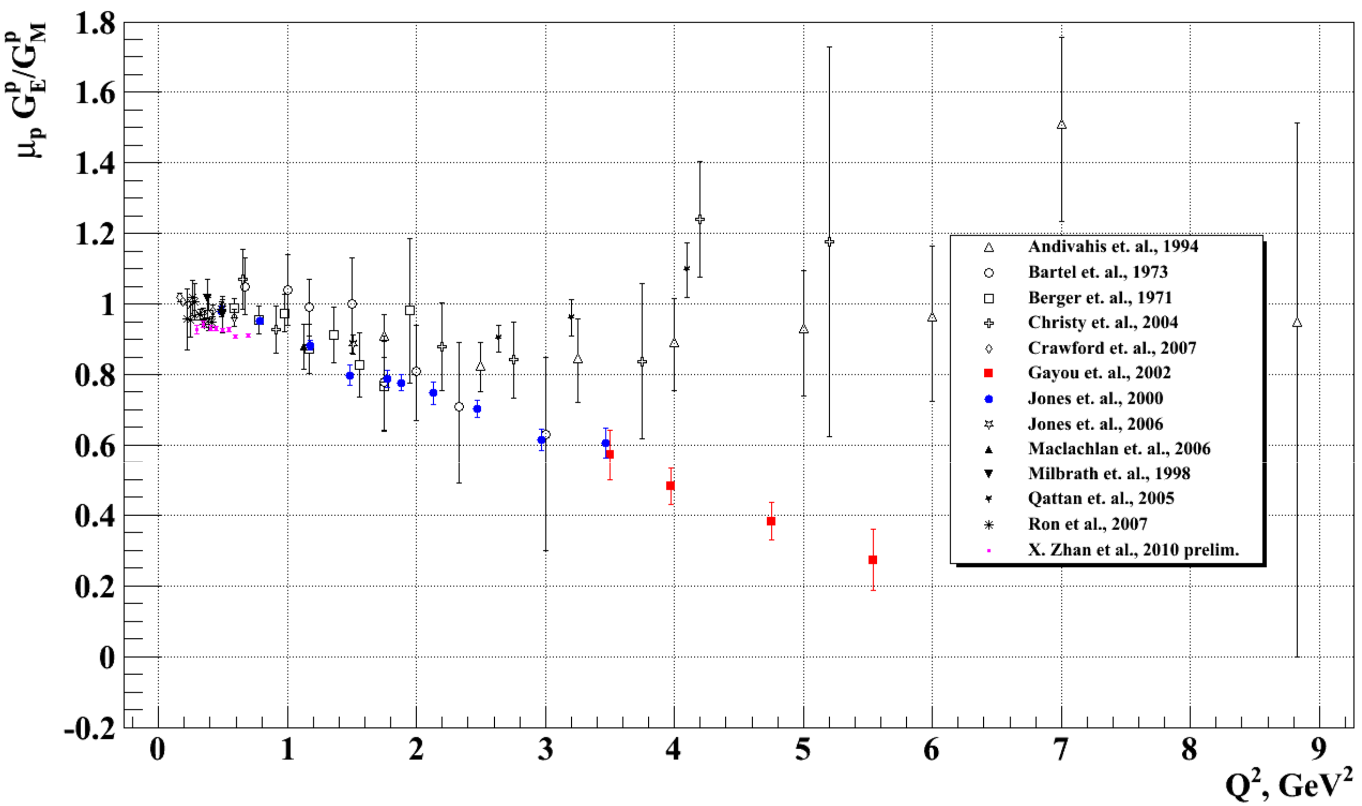

Precise recoil polarization data for $R=\mu_p G_E^p/G_M^p$ conclusively revealed a strong deviation from $R \approx 1$ scaling of cross section data

Jefferson Lab/CEBAF/TJNAF

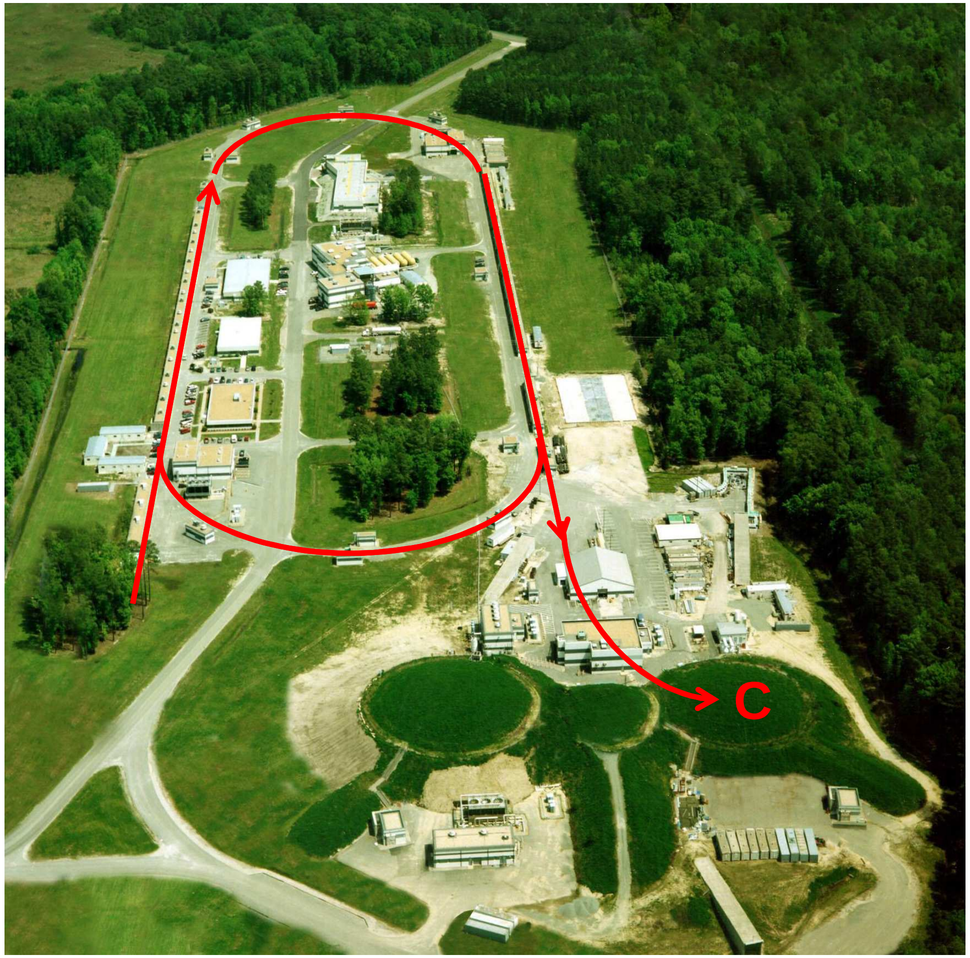

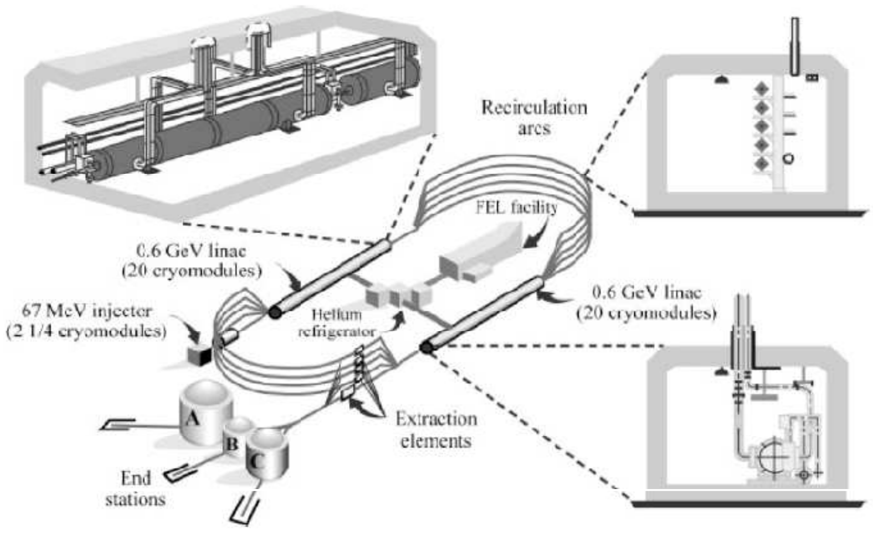

Figure 3-1: Schematic of the CEBAF accelerator

Experiments E04-108 & E04-019

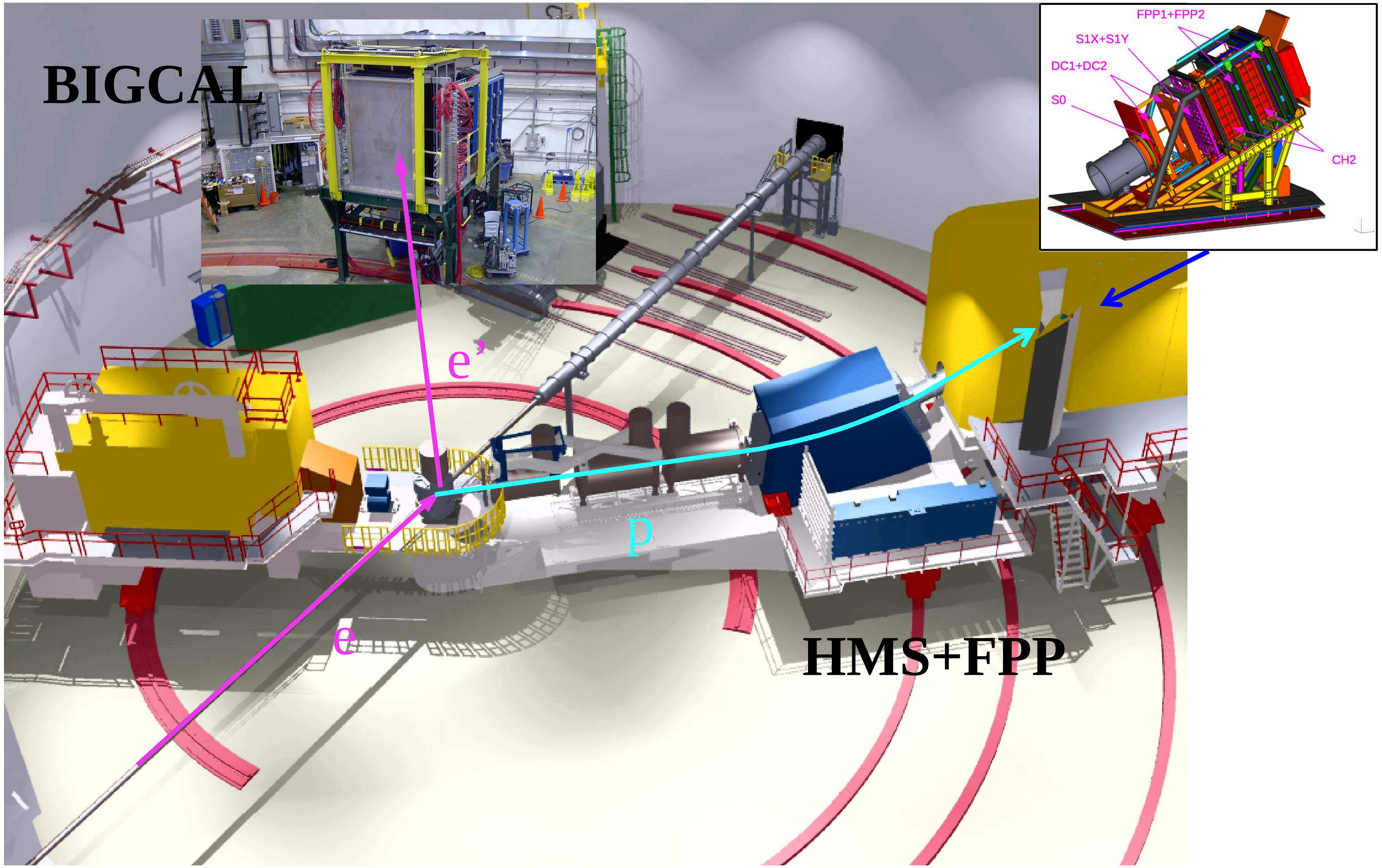

New recoil polarization measurements of G_E^p/G_M^p in Hall C at JLab

Kinematics

Q^2, GeV^2	ε	E_{beam}, GeV	θ_p, °	p_p, GeV	E_e, GeV	θ_e,°
2.5	0.154	1.873	14.495	2.0676	0.532	105.2
2.5	0.633	2.847	30.985	2.0676	1.51	44.9
2.5	0.789	3.680	36.10	2.0676	2.37	30.8
5.2	0.377	4.053	17.94	3.5887	1.27	60.3
6.8	0.507	5.714	19.10	4.4644	2.10	44.2
8.5	0.236	5.714	11.6	5.407	1.16	69.0

- E04-108: three new high Q^2 measurements
- E04-019: precision measurements at Q^2=2.5 GeV^2 for three ε values; look for signatures of TPEX
- Beam: ~60-100 µA CW, 80-85% polarized (Moller)
- Target: 20 cm LH_2, nominal luminosity ~4 × 10^{38} $s^{-1}cm^{-2}$

HMS+FPP

- High Momentum Spectrometer (HMS), superconducting, 25° vertical bend magnetic spectrometer measures proton:
  - Angles
  - Momentum
  - Vertex
- Focal Plane Polarimeter:
  - Measure transverse components of proton polarization at the focal plane

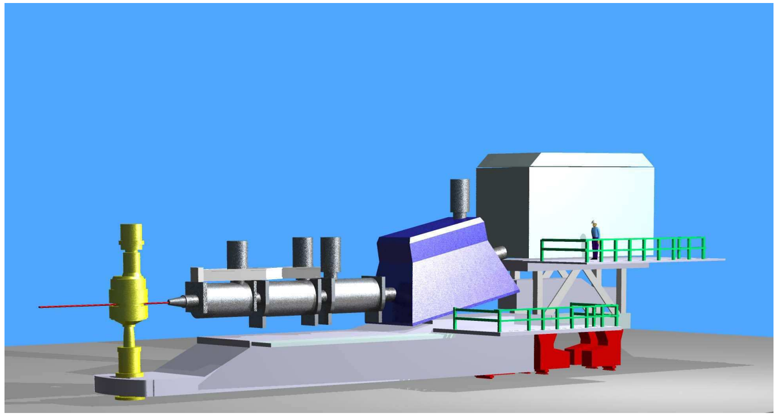

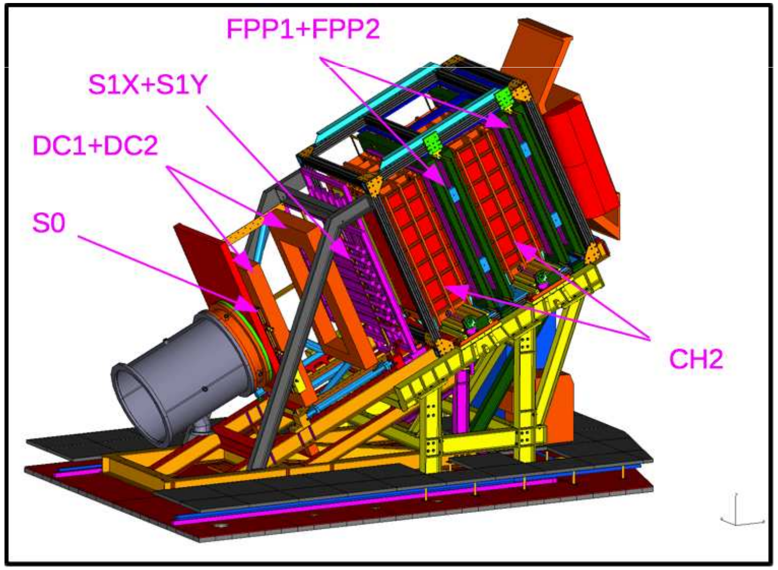

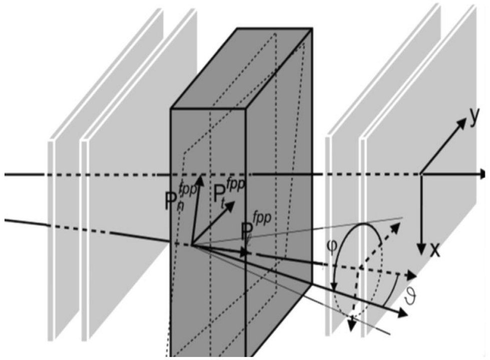

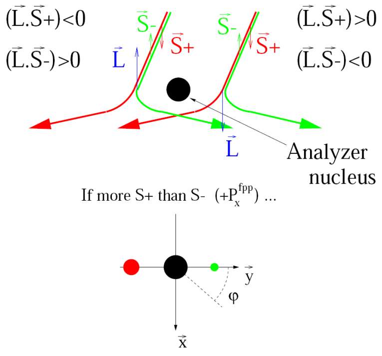

BigCal

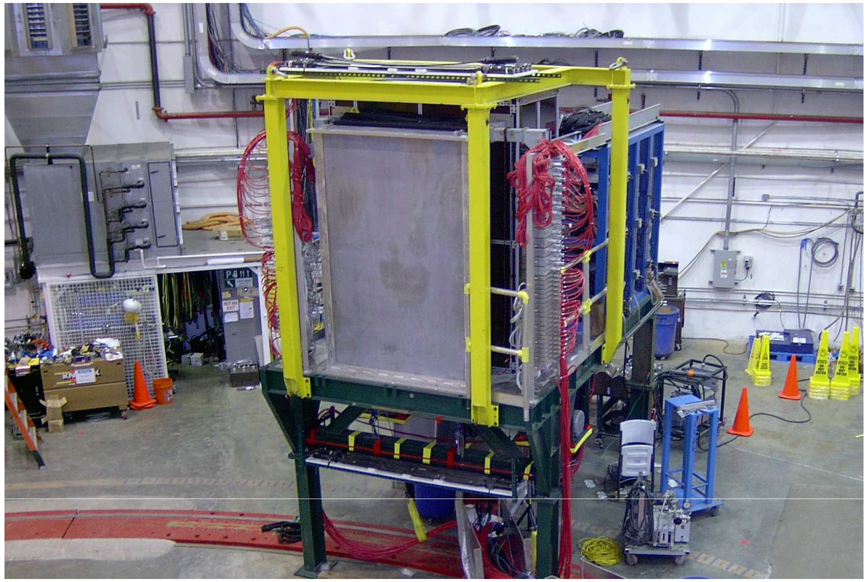

- Measure electron angles, energy
- Separate elastic from inelastic using angular correlation
- Large Jacobian in elastic ep scattering—large acceptance to match proton arm
- For $Q^2 = 8.5\ \mathrm{GeV}^2$, $\Omega_e = 143$ msr to $\Omega_p = 6.7$ msr

Data Analysis

- Elastic Event Selection
  - Inelasticity variable definitions
  - Cut selection and background estimation
- Extraction of Polarization Observables
  - Focal plane asymmetry extraction
  - Spin precession calculation

Elastic Event Selection, I

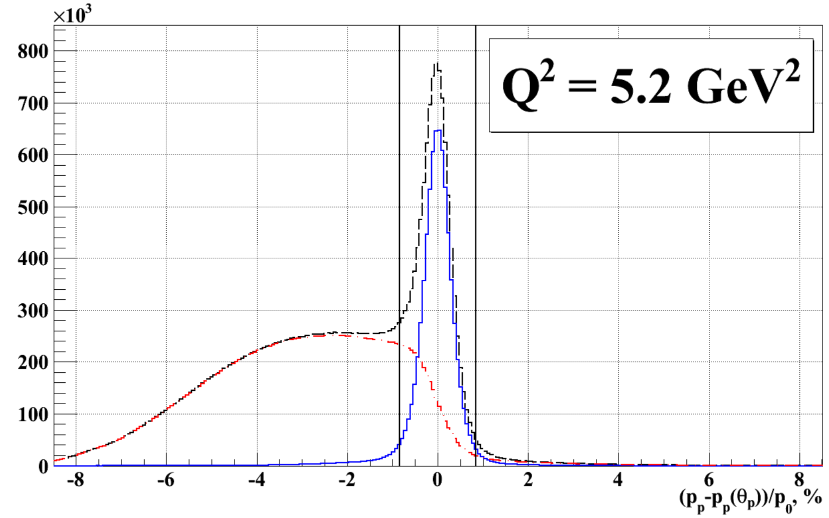

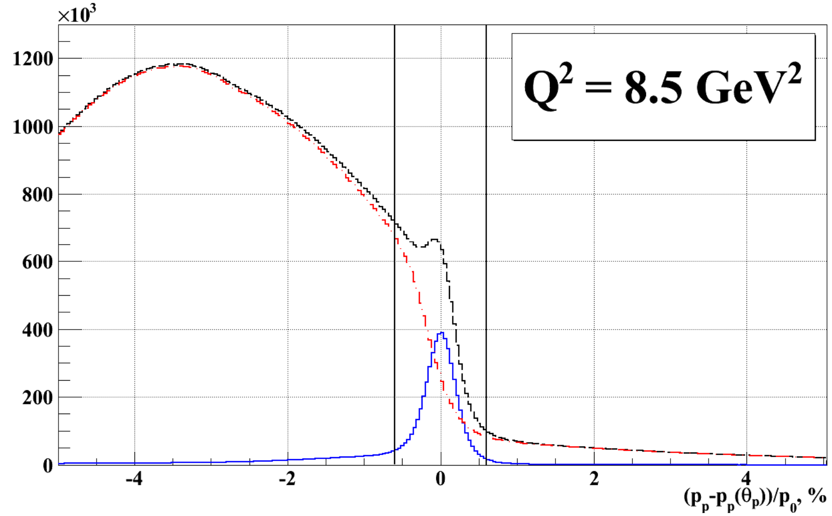

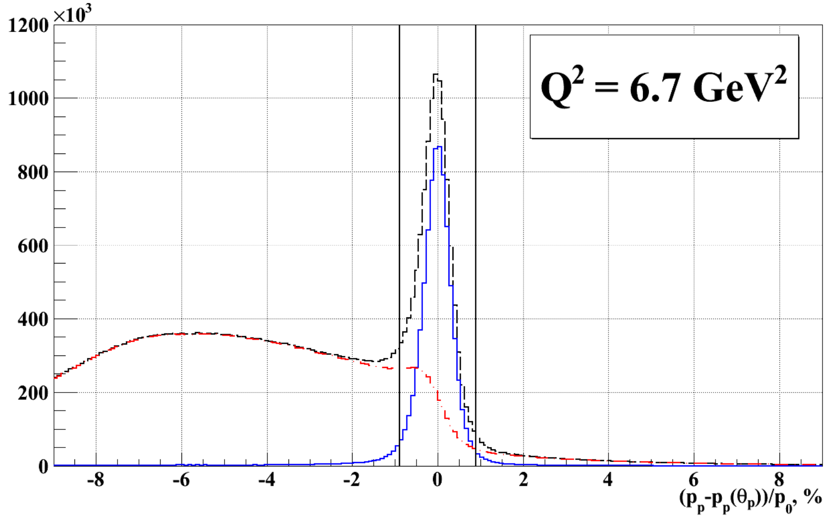

$$p_p(\theta_p) = \frac{2M_p E_e (E_e + M_p)\cos\theta_p}{M_p^2 + 2M_p E_e + E_e^2 \sin^2\theta_p}$$

- Proton angle-momentum correlation in elastic scattering
- p-p(θ) spectra:
  - ALL/PASS/FAIL cuts

Elastic Event Selection, II

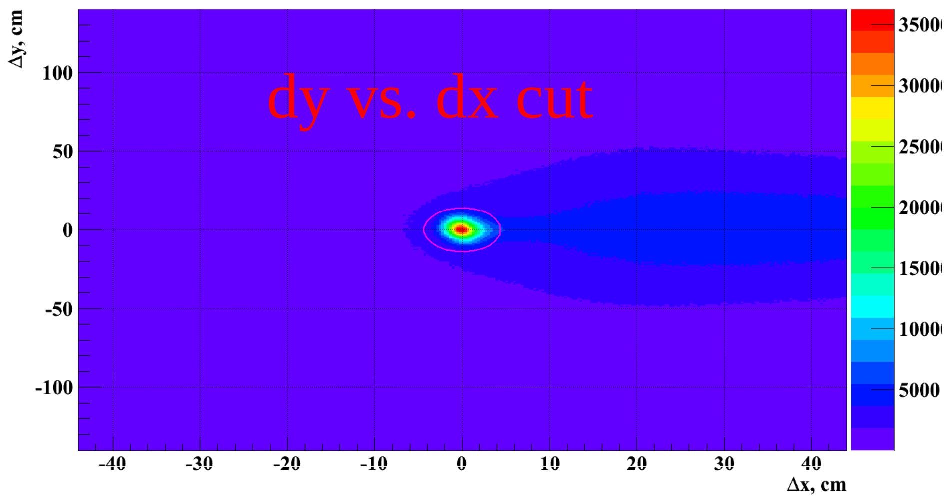

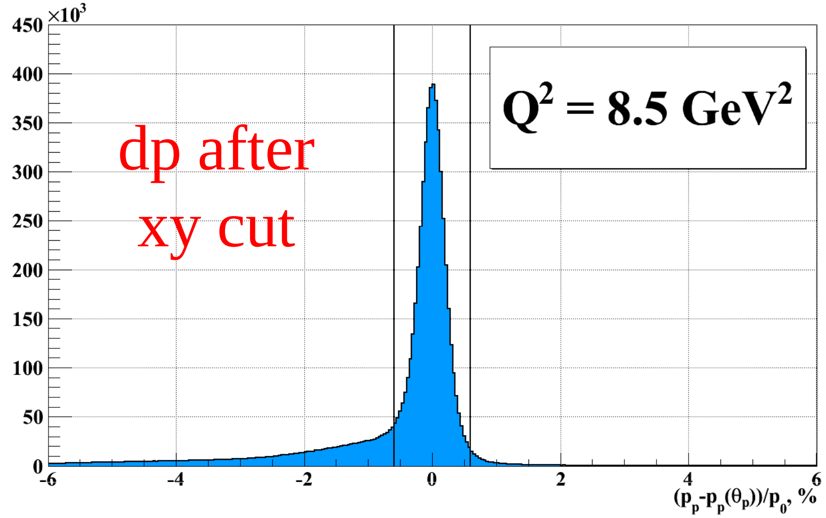

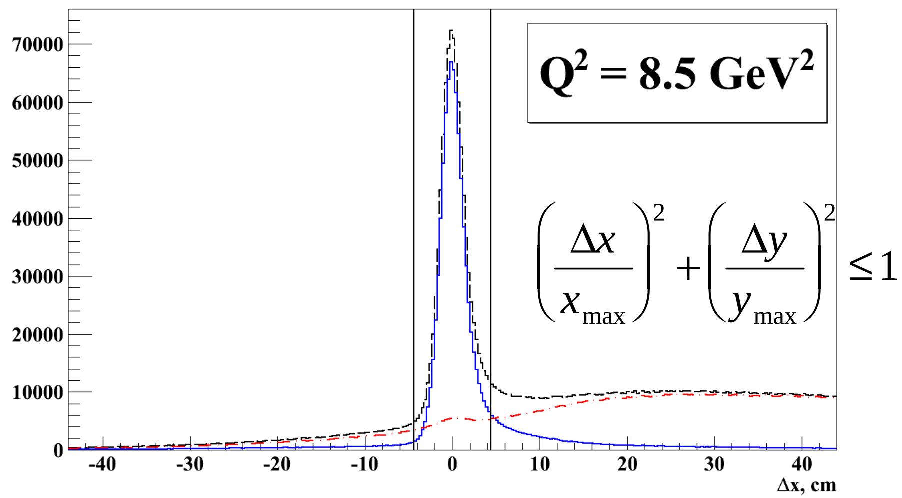

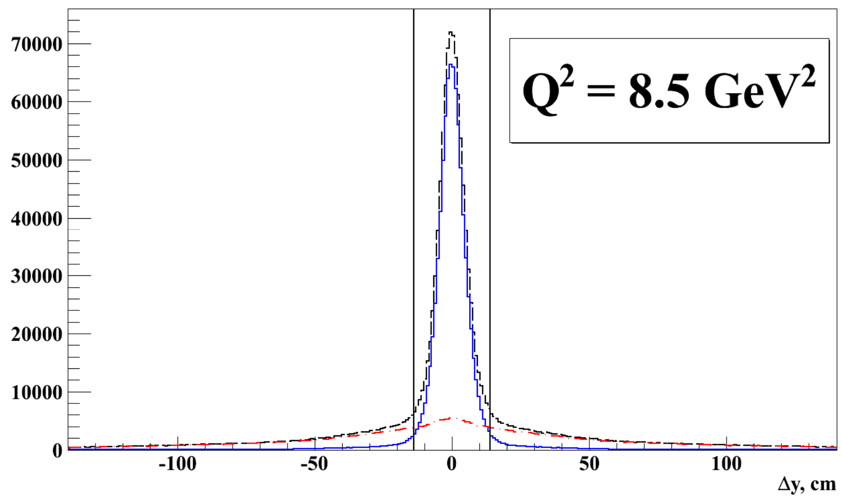

Background Estimation

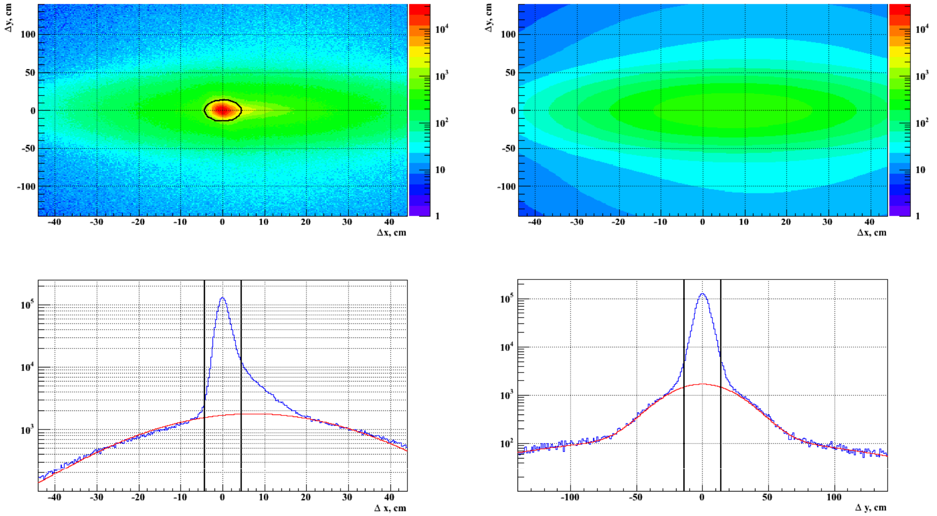

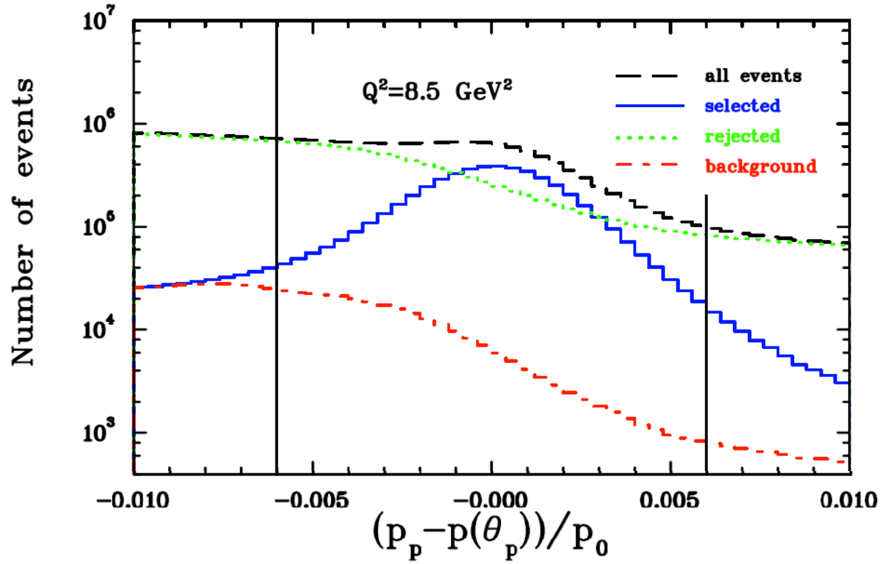

- Estimate background directly from data by extrapolating dx, dy distribution under the peak (above):
  - Data, fitted background and projections
- Compare data (top right) and MC (bottom right) for dp

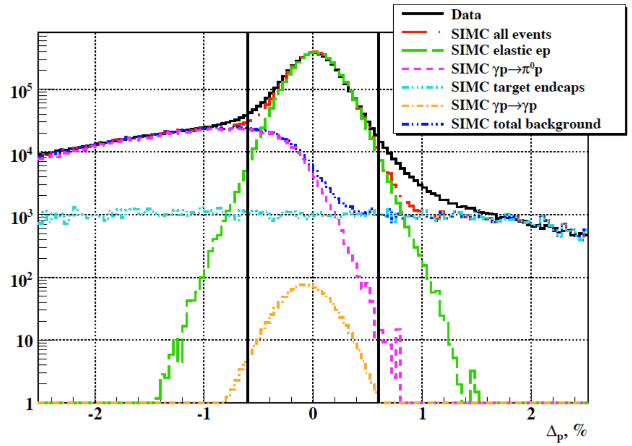

Background Subtraction

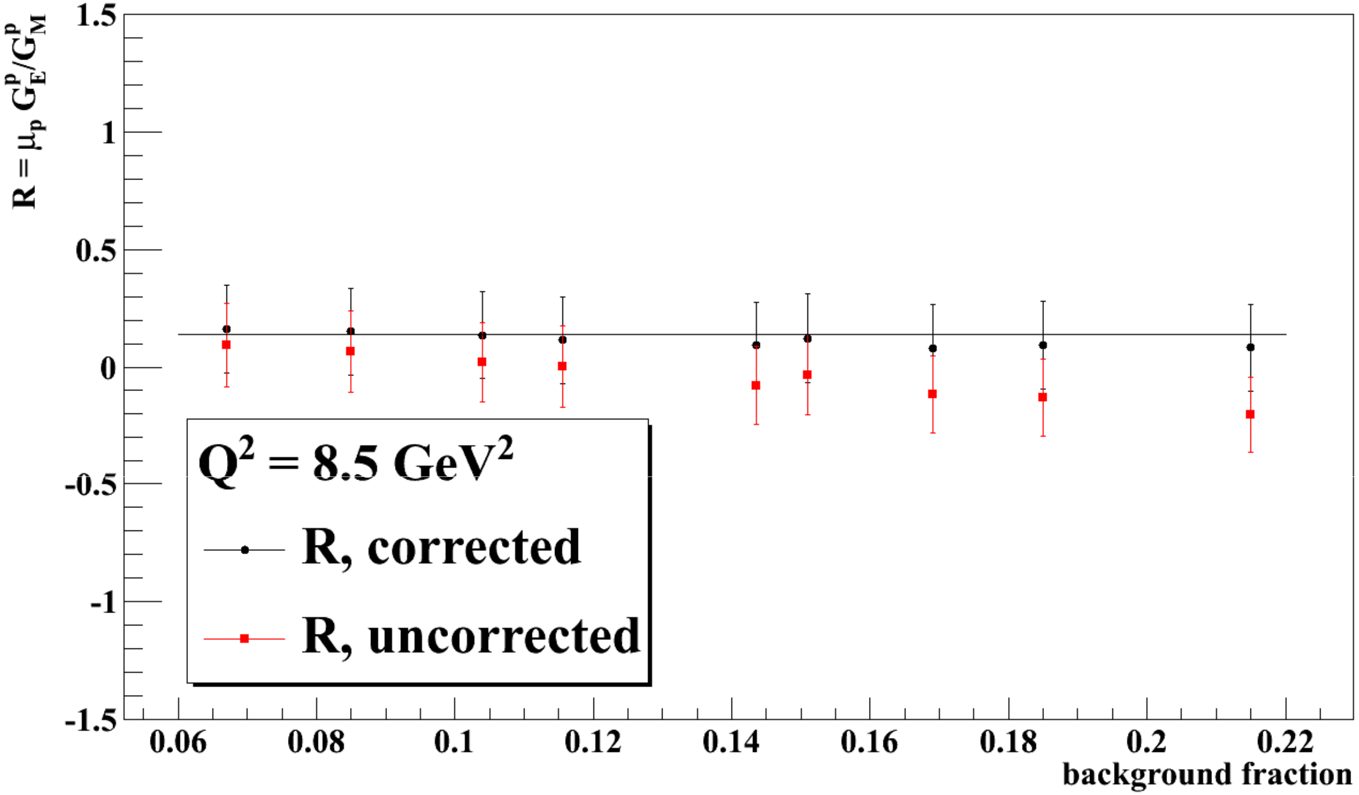

$$f = \frac{N_{inel.}}{N_{el.} + N_{inel.}}$$

$$P_{obs} = (1 - f)P_{el} + fP_{inel}$$

$$P_{el} = \frac{P_{obs} - fP_{inel}}{(1 - f)}$$

- Background and signal polarizations differ, F. F. ratio decreases as elastic cuts are relaxed
- Stability of background-subtracted F. F. ratio w.r.t. cut variations including more background validates background subtraction method

Extraction of Polarization Observables

$$N^{\pm}(\vartheta,\varphi) = N_0^{\pm}\frac{\varepsilon(\vartheta)}{2\pi}\begin{bmatrix} 1+\left(c_1(\vartheta)\pm A_y(\vartheta)P_y^{fpp}\right)\cos\varphi \\ +\left(s_1(\vartheta)\mp A_y(\vartheta)P_x^{fpp}\right)\sin\varphi + \\ c_2(\vartheta)\cos(2\varphi)+s_2(\vartheta)\sin(2\varphi)+\ldots \end{bmatrix}$$

$$f_{\pm} = \frac{N^{\pm}(\vartheta,\varphi)}{N_0^{\pm}}$$

$$f_+ + f_- = \frac{\varepsilon(\vartheta)}{\pi}\begin{bmatrix} 1+c_1\cos\varphi+s_1\sin\varphi+ \\ c_2\cos(2\varphi)+s_2\sin(2\varphi)+\ldots \end{bmatrix}$$

$$f_+ - f_- = \frac{\varepsilon(\vartheta)A_y(\vartheta)}{\pi}\left[P_y^{fpp}\cos\varphi - P_x^{fpp}\sin\varphi\right]$$

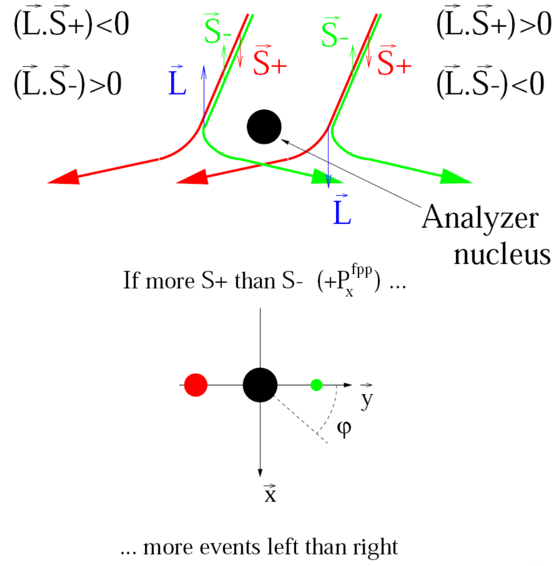

Angular distribution and azimuthal asymmetry definitions

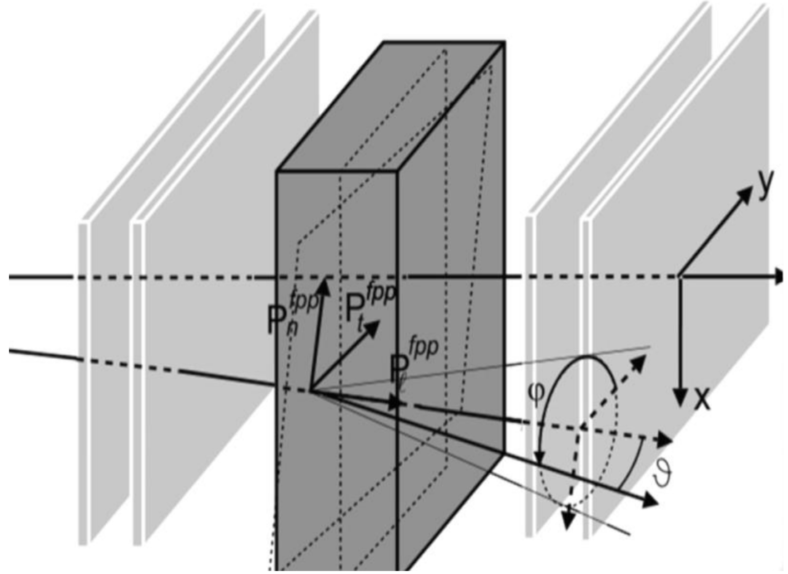

Polarization Observables—FPP Asymmetry

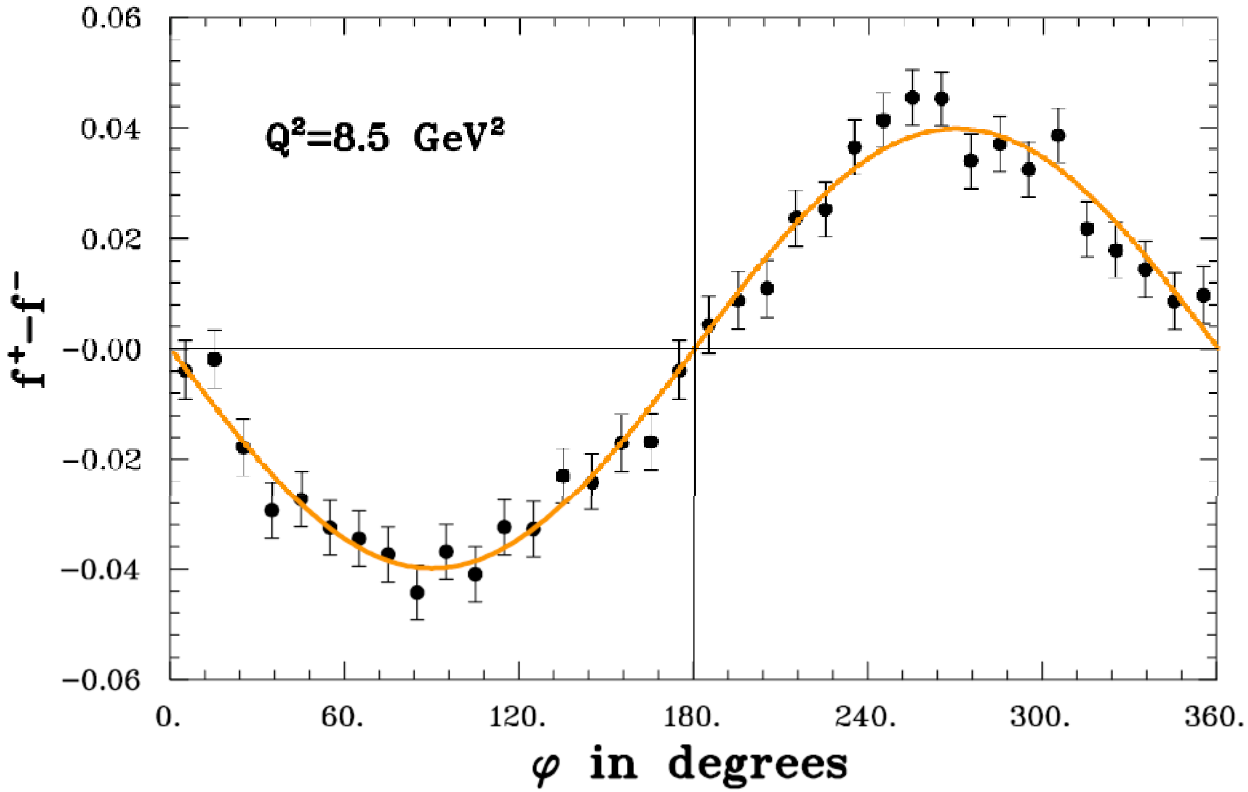

$$f_+ - f_- = A\sin(\varphi + \delta)$$

$$A = \overline{A_y}\sqrt{\left(P_x^{fpp}\right)^2 + \left(P_y^{fpp}\right)^2}$$

$$\tan\delta = -\frac{P_y^{fpp}}{P_x^{fpp}}$$

Helicity difference asymmetry, $Q^2 = 8.5$ GeV^2, $0.5° \leq \theta \leq 14.0°$

Polarization Observables—FPP Asymmetry

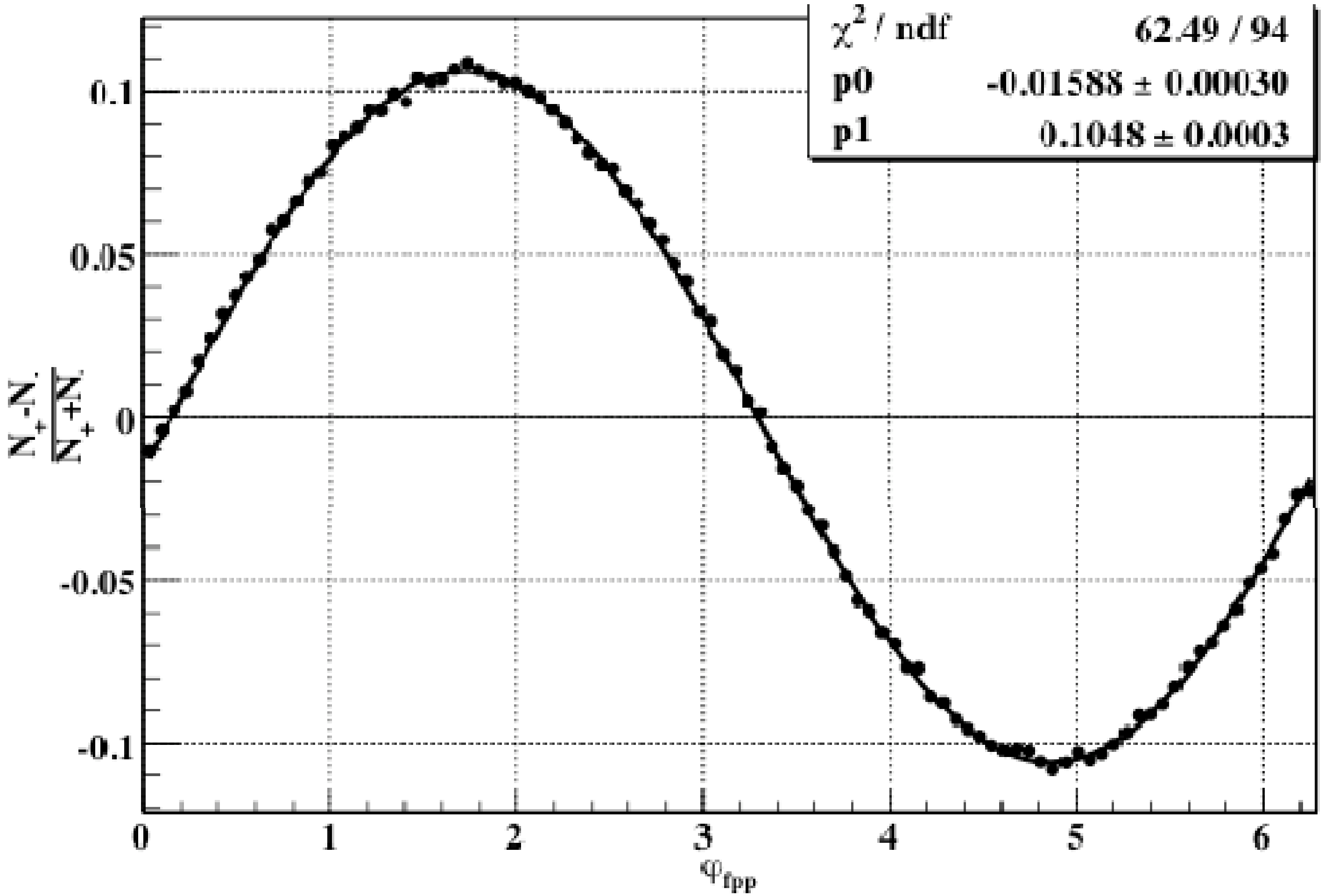

FPP asymmetry, Q^2=2.5 GeV^2, ε=0.15

Spin Precession, I

$$\frac{d\vec{S}}{dt} = \frac{e}{m\gamma}\vec{S}\times\left[\frac{g}{2}\vec{B}_{\parallel} + \left(1+\gamma\left(\frac{g}{2}-1\right)\right)\vec{B}_{\perp}\right]$$

$$\frac{d\vec{v}}{dt} = \frac{e}{m\gamma}\vec{v}\times\vec{B}$$

$$\left(\frac{d\vec{S}}{dt}\right)_{comoving} \xrightarrow{B_{\parallel}=0} \gamma\left(\frac{g}{2}-1\right)\frac{e}{m\gamma}\vec{S}\times\vec{B}$$

$$\chi = \gamma\kappa\theta_{bend}$$

Q^2, GeV^2	p_0, GeV/c	χ_θ, °
2.5	2.0676	108.5
5.2	3.5887	177.2
6.7	4.4644	217.9
8.5	5.4070	262.2

- BMT equation (1959): relativistic spin precession in a magnetic field
- χ = precession angle relative to velocity in a constant, uniform magnetic field
- Precession angles corresponding to HMS 25° central bend for this experiment shown in table
- Unique spin rotation for each event, calculated using HMS COSY model

Spin Precession, II

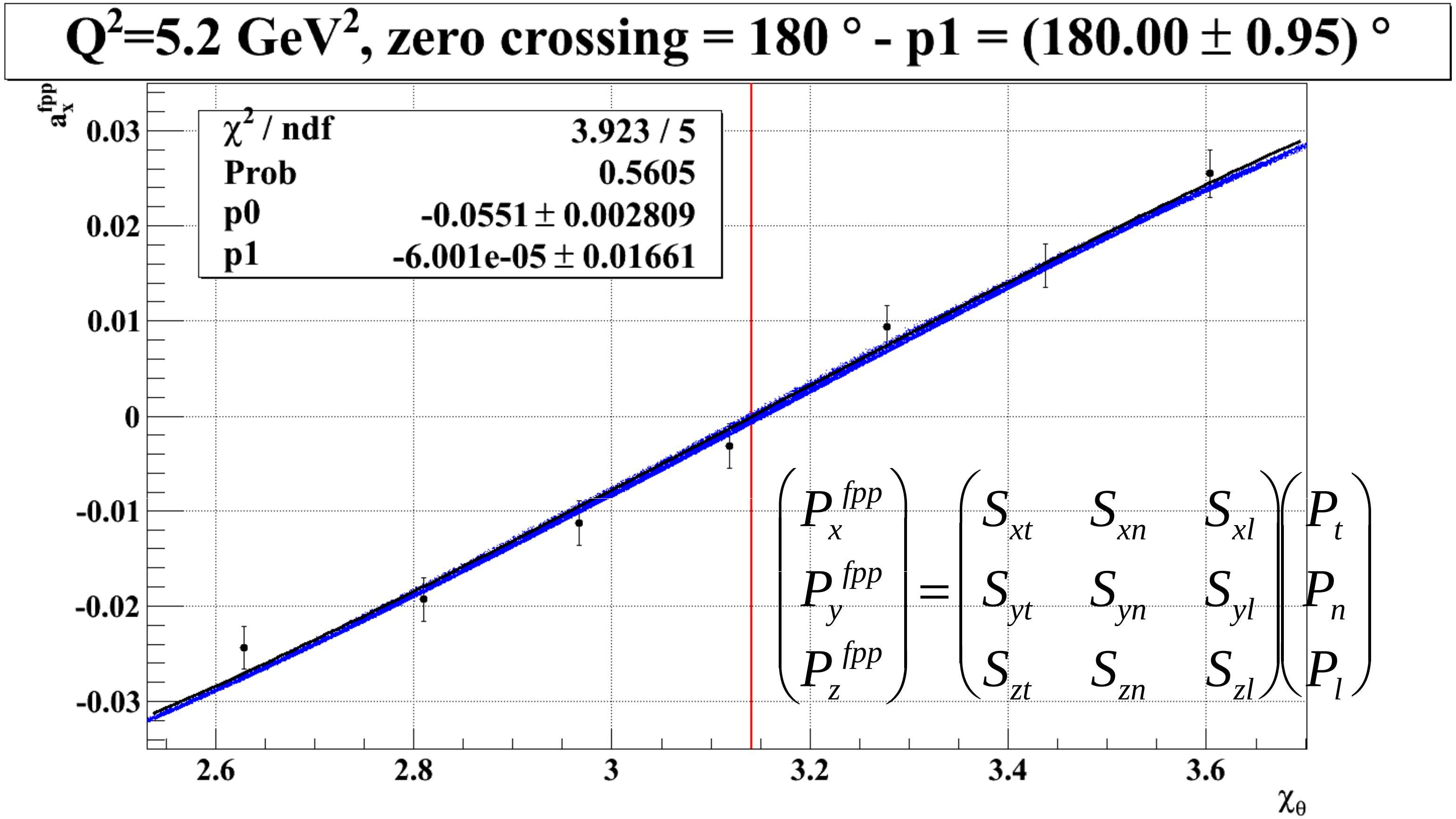

- Normal asymmetry at focal plane should cross zero at χ=180°
- Within statistics, data compatible with this prediction
- Fit: $a_x = p0 \sin(\chi+p1)$, $\langle hA_y \rangle S_{xl} P_l$ from COSY agrees with χ-dependence of the data

Spin Precession, III

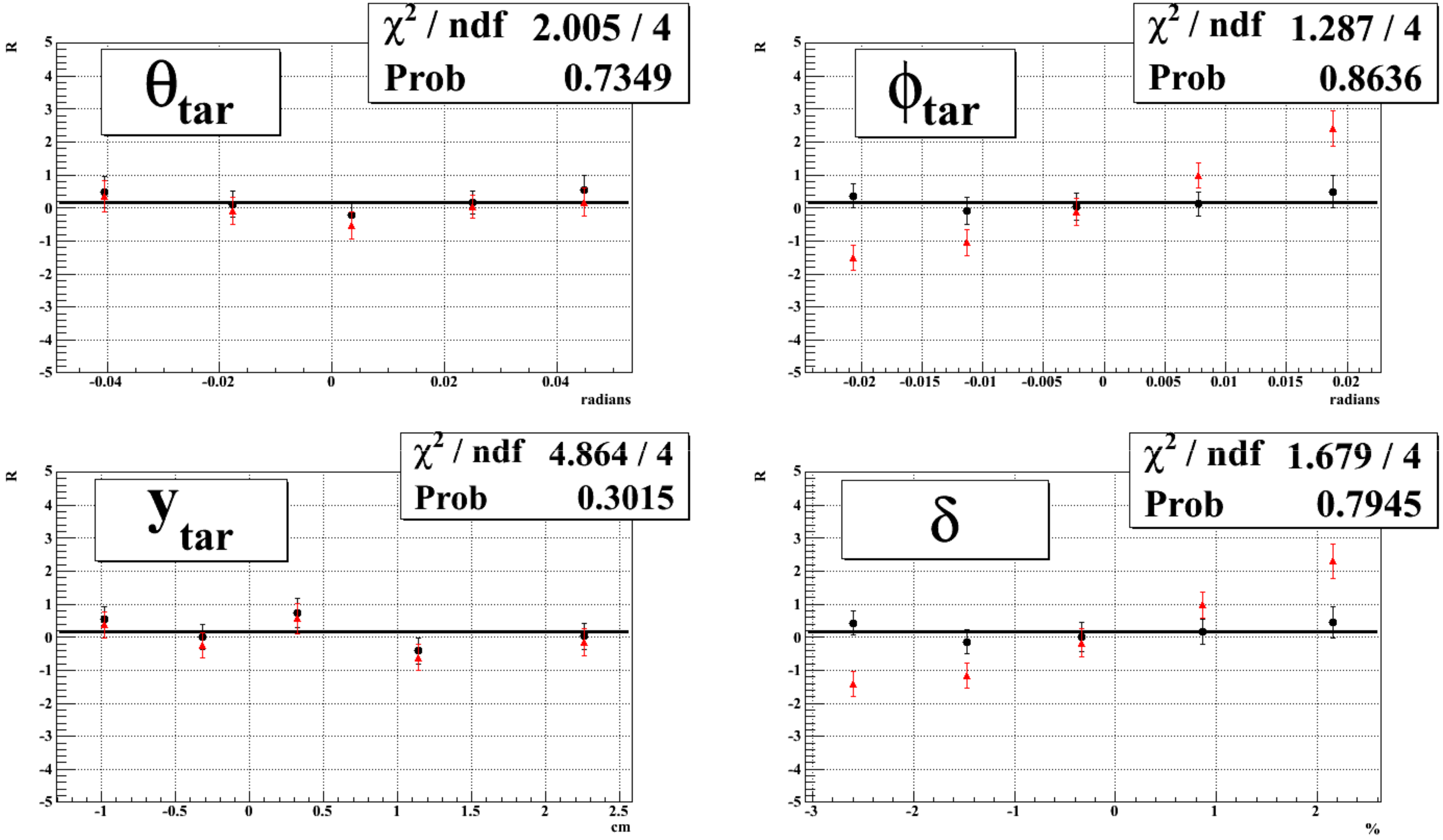

R vs. reconstructed kinematics, **$Q^2 = 8.5$ GeV^2, DIPOLE/COSY**

Spin Precession, IV

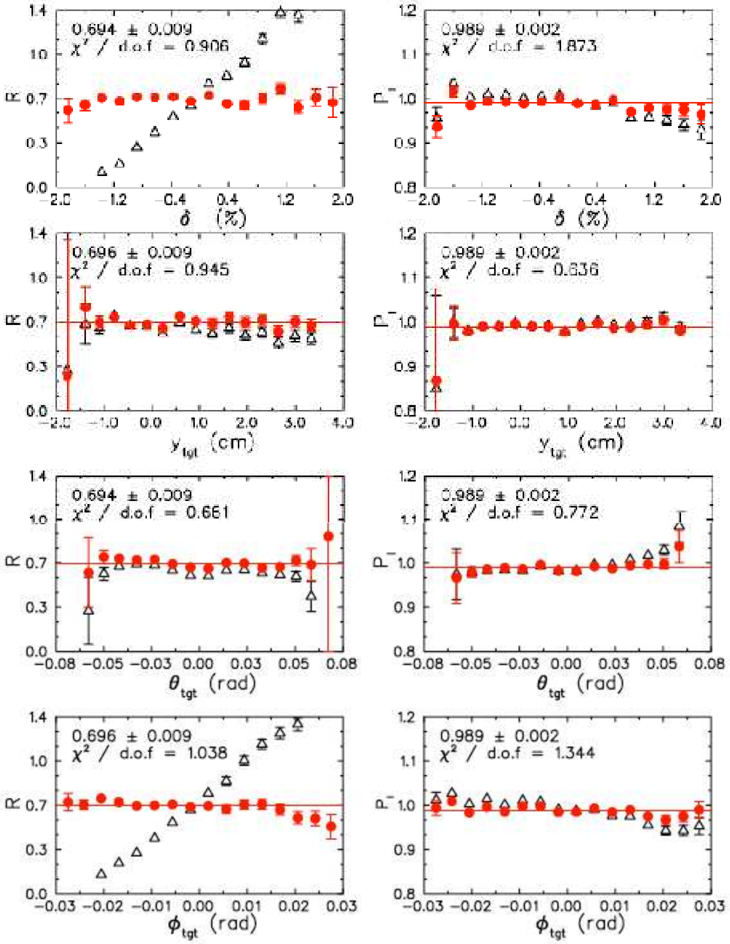

R and P_l/P_l(Born) vs. reconstructed kinematics
DIPOLE/COSY, Q^2=2.5 GeV^2, ε=0.15

- High-precision data at Q^2=2.5 GeV^2 provide a strong test of spin transport calculation.
- Benchmark test: extracted form factor ratio is independent of reconstructed kinematics
- χ^2 of constant fit close to one for all four target variables:
  - δ = percent deviation from central momentum
  - θ_{tar}= vertical angle
  - ϕ_{tar}= horizontal angle
  - y_{tar} = vertex
- P_t, P_l and R can vary across acceptance due to finite spectrometer acceptance.
  - Effects generally small, especially for R
  - Effects on P_t, P_l larger at small ε

Systematic Uncertainties, GEp-III

Q^2, GeV^2	5.2	6.7	8.5
ϕ_{bend} (±.5 mrad)	.0162	.0202	.0378
θ_{bend} (±2 mrad)	.0009	.0006	.0002
δ (±0.3%)	.0029	.0027	.0024
φ_{fpp} (±.14 mrad/sin(ϑ_{fpp}))	.0003	.0057	.0178
E_{beam} (±.05%)	.00027	.00009	.00025
False asym.	.0069	.0057	.0018
Background	.0015	.0013	.0130
Rad. Corr. (% of R)	0.05% ($\Delta R \approx$ -.0002)	0.12% ($\Delta R \approx$ -.0004)	0.13% ($\Delta R \approx$ -.0002)
Total ΔR_{syst}	.018	.022	.043

- Non-dispersive precession uncertainty dominates the systematic uncertainty in R
- **A_y, h cancel**, no uncertainty for R
- Standard radiative corrections (not applied) **negligible** compared to other uncertainties

E04-108 Final Results, I

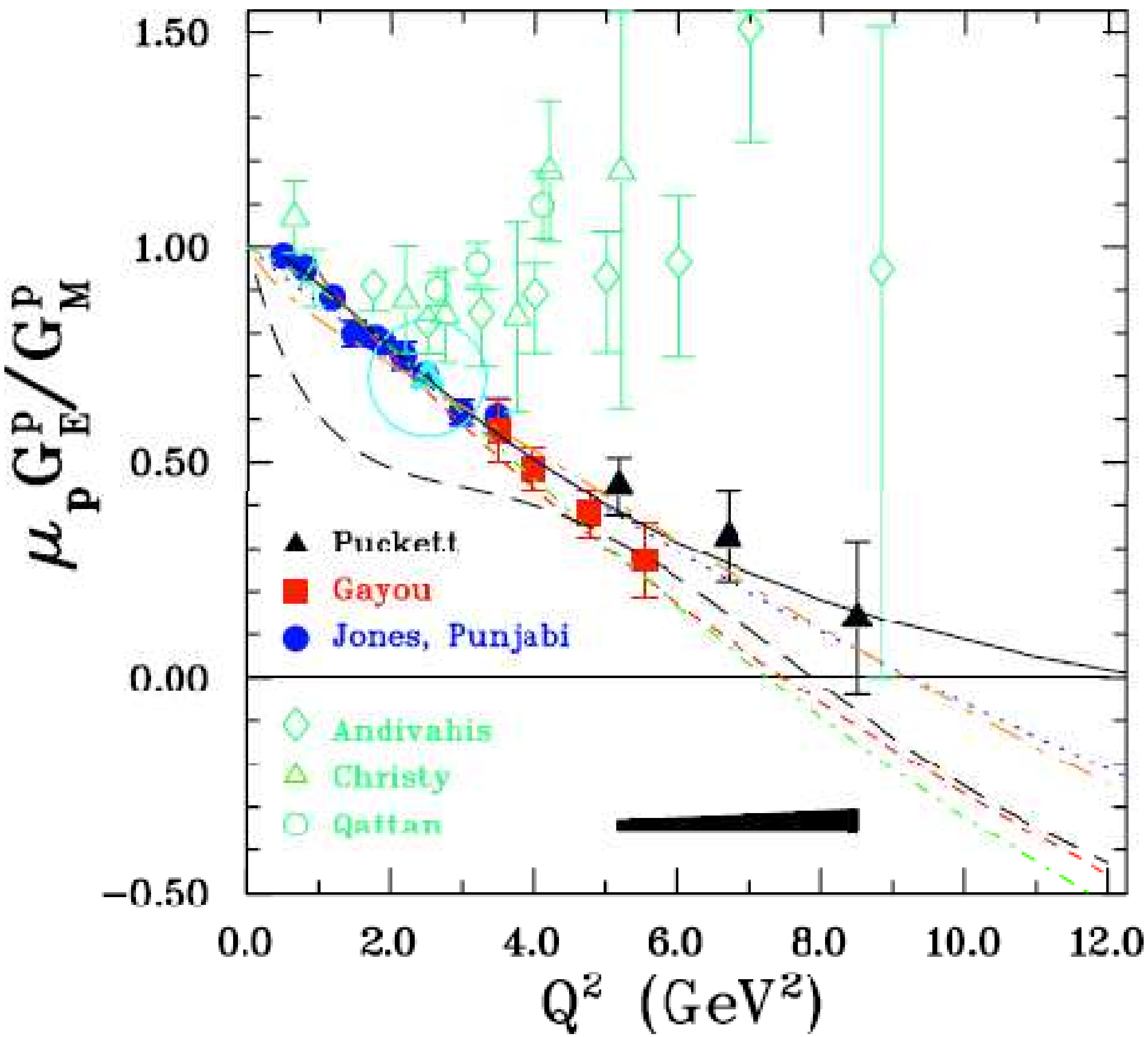

- Results published A. J. R. Puckett et al., **PRL 104, 242301 (2010)**
- 50% increase in Q^2 coverage
- New data favor a slowing rate of decrease of R
- **GEp-2γ (preliminary, averaged over ε)**

E04-108 Final Results, II

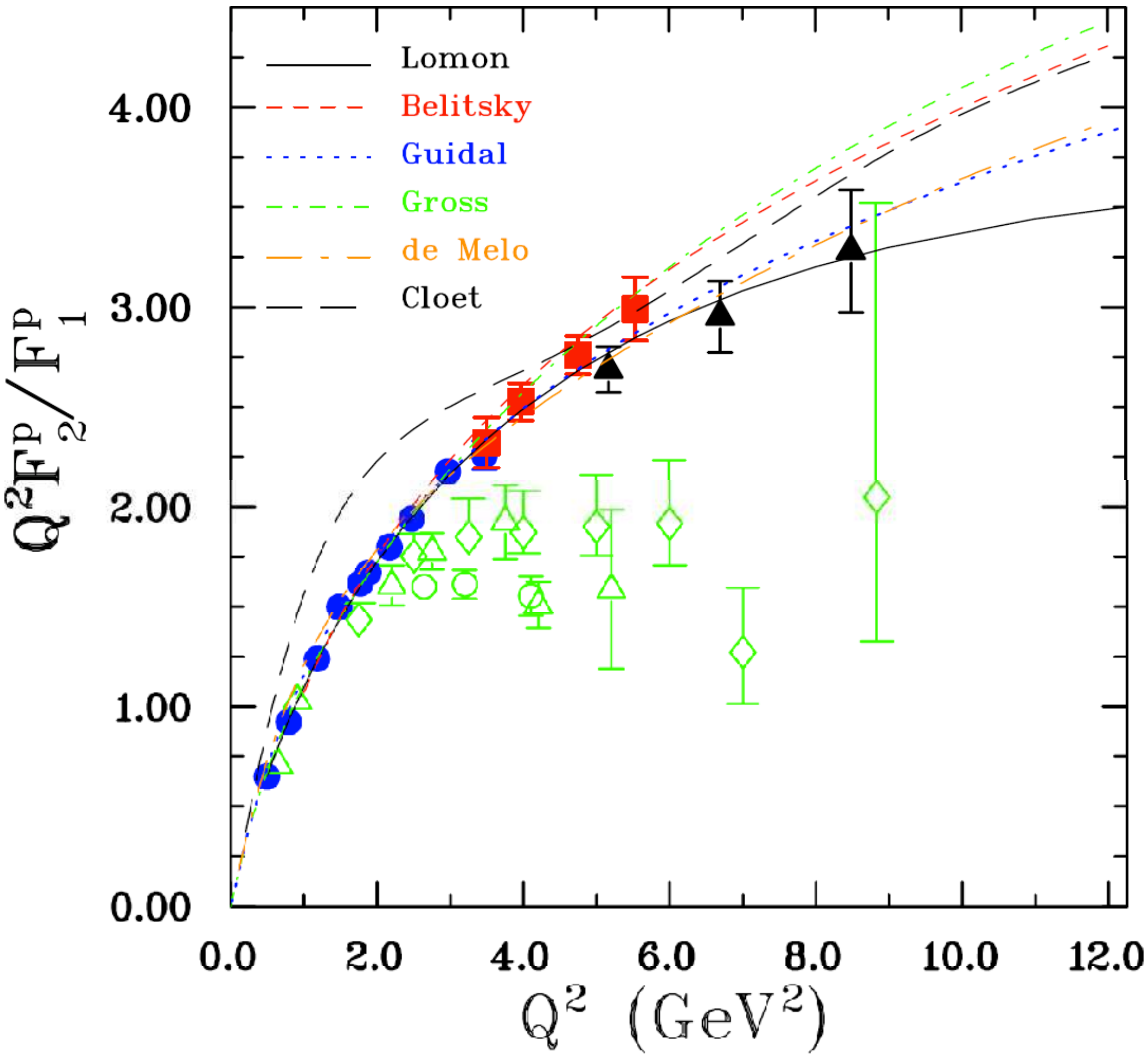

- **Theory curves:**
- Lomon 2002, 2006 (VMD)
- Belitsky 2003 (pQCD scaling)
- Guidal 2005 (GPD)
- Gross, Ramalho, Pena 2008 (covariant spectator model)
- de Melo 2009 (Bethe-Salpeter Amplitude)
- Cloet 2009 (Dyson-Schwinger/Faddeev/quark-diquark)

E04-019 Preliminary Results

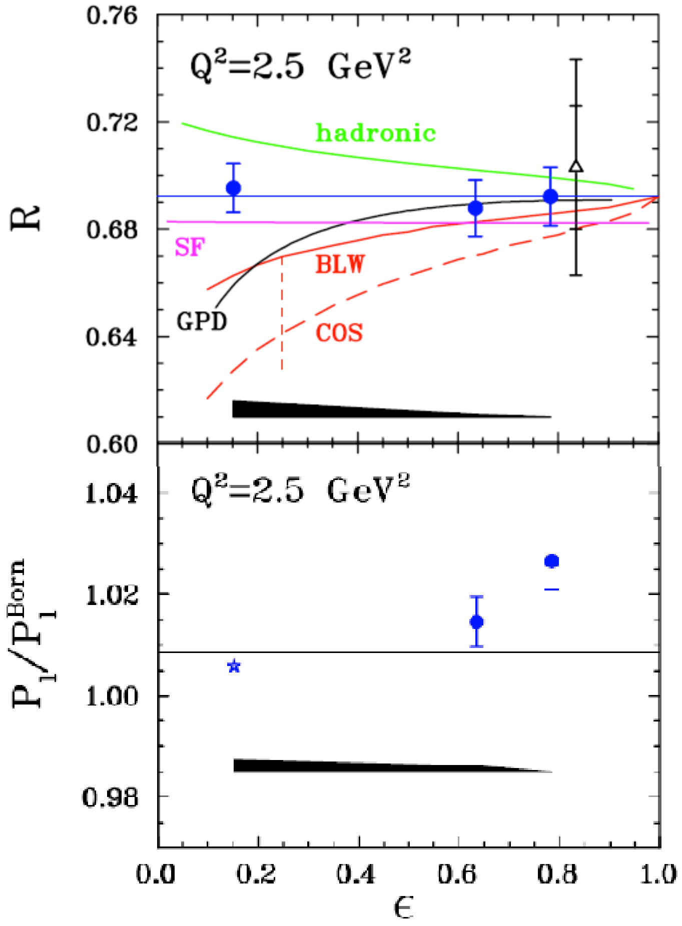

- Two high-ε kinematics cut to the same acceptance as lowest ε:
  - Same Q^2 acceptance
  - Same spin transport systematics
- No significant ε dependence of R at Q^2=2.5 GeV^2 extracted from polarization transfer
- Strong constraint on TPEX amplitudes in elastic ep scattering, severely restrict available calculations
- P_l/P_l(Born) shows an increase with ε, with a few σ significance
- Several assumptions built into extraction of absolute P_l

Theory Overview—G_{Ep}

VMD

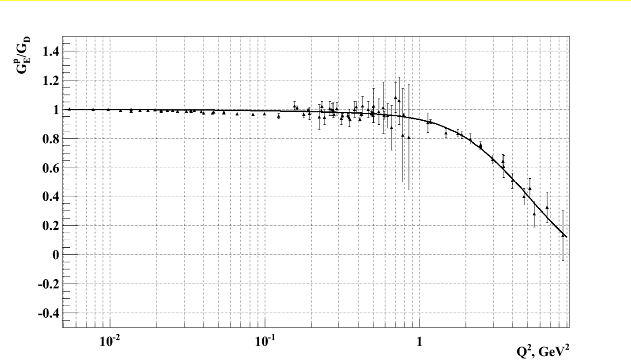

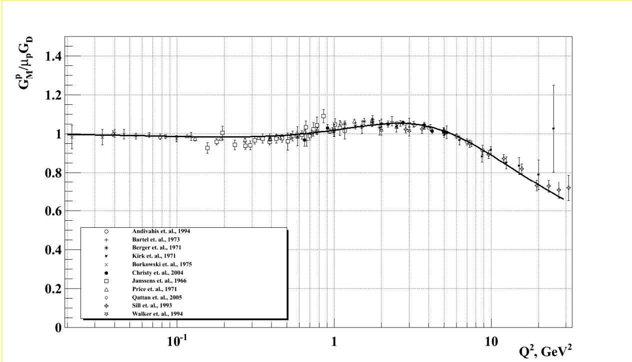

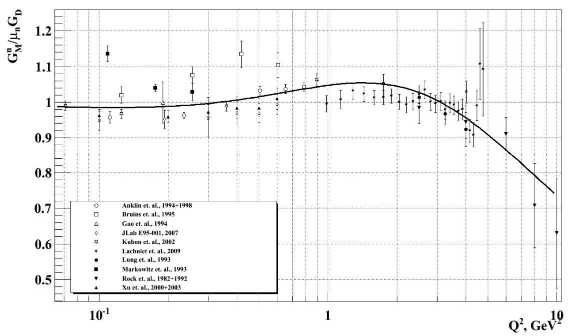

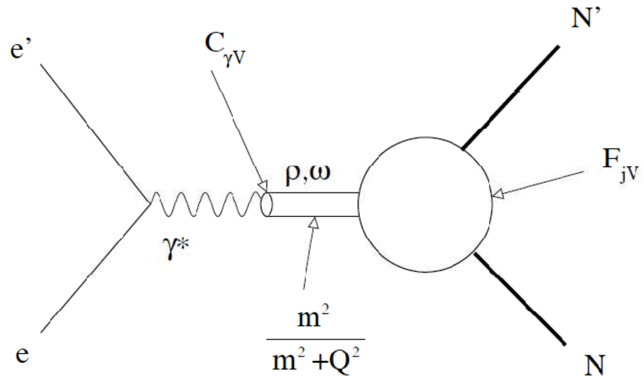

$$F(q^2) = \frac{1}{\pi}\int_{t_0=4m_\pi^2}^{\infty}\frac{\mathrm{Im}F(t)}{(t-q^2)}dt$$

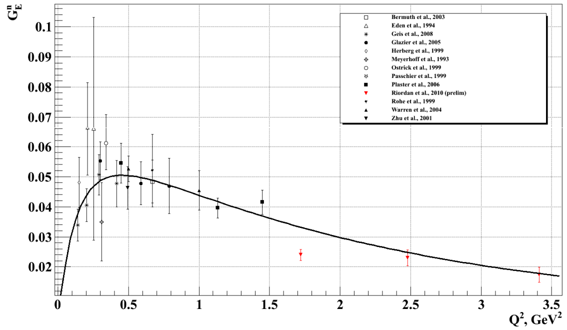

- Fits by Lomon in extended Gari-Krumpelmann model, nucl-th/0609020
- ρ, ω, ϕ, ρ', ω' mesons + "direct coupling" enforces pQCD asymptotic behavior

Bethe-Salpeter Amplitude

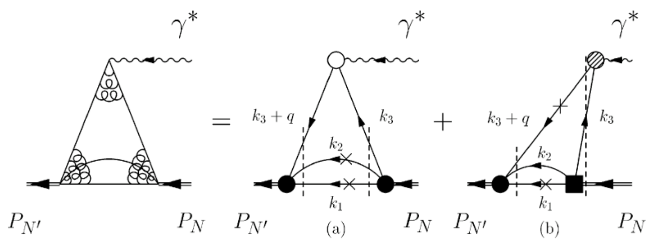

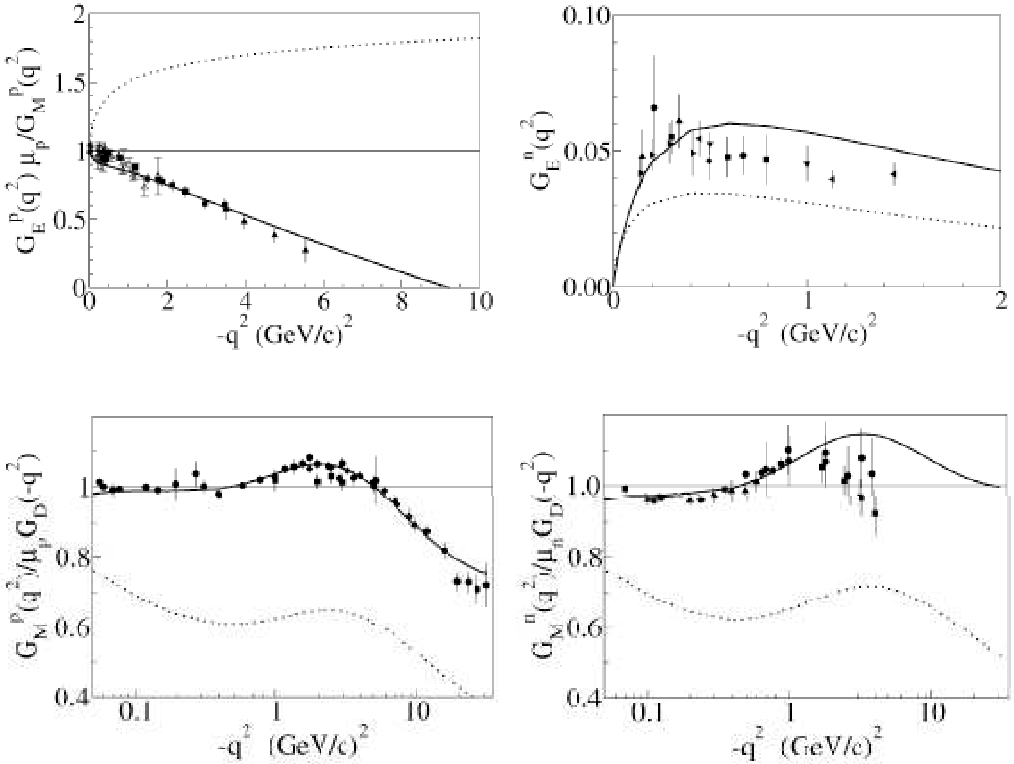

- Combined Ansatz for nucleon Bethe-Salpeter amplitude and microscopic VMD model, consider valence and non-valence components of the nucleon state in light-front dynamics

de Melo et al. PLB 671, 153 (2009)

GPDs, I

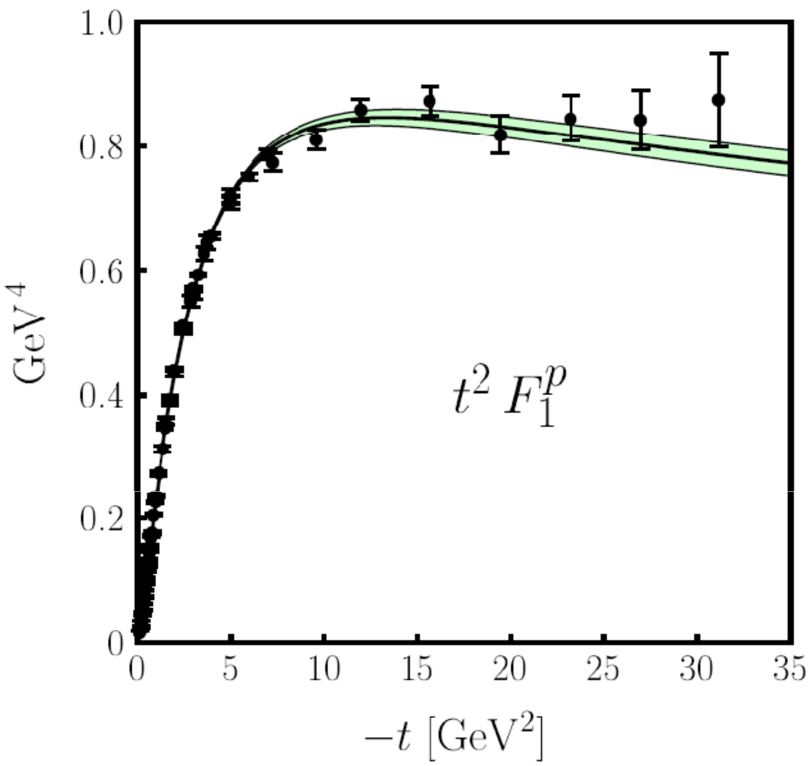

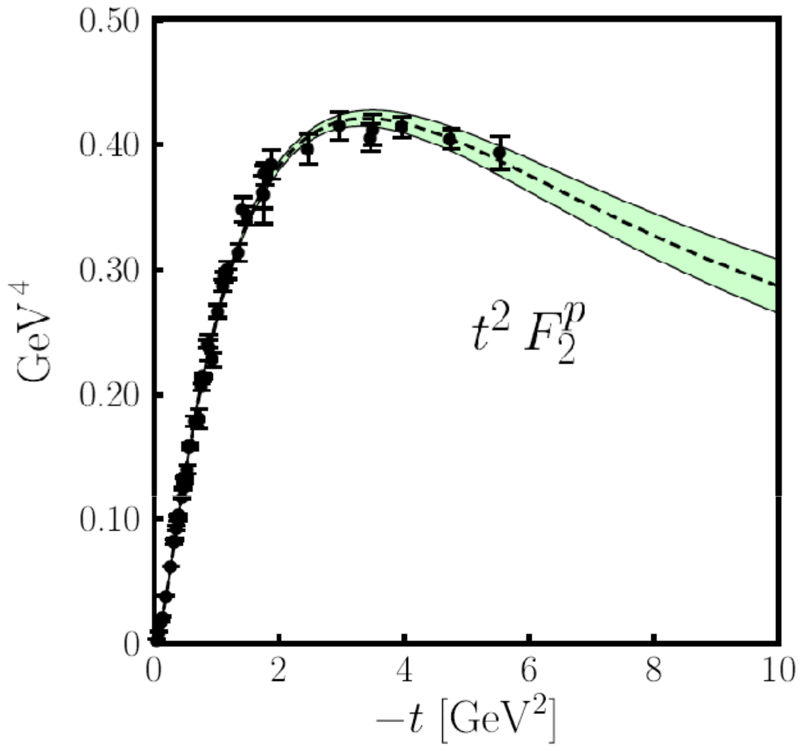

$$\int_{-1}^{1} dx H^q(x,\xi,t) \;=\; F_1^q(t)$$
$$\int_{-1}^{1} dx E^q(x,\xi,t) \;=\; F_2^q(t)$$

- Form factors constrain GPDs through sum rules: 0th moments of vector (H) and tensor(E) GPDs equal e.m. form factors
- Above: Diehl et al; EPJ C, 39, 1 (2005)

GPDs, II

- Guidal et al., PRD 72, 054013 2005: Modified Regge parametrization of valence quark GPDs
- Three-parameter fit to nucleon form factor data
- Constraint on E from precise $\boldsymbol{F_{2p}}$ data allowed evaluation of Ji sum rule:

$$2J^q = \int_{-1}^{1} dx x\{H^q(x,0,0) + E^q(x,0,0)\},$$

	M_2^q (MRST2002)	$2J^q$ (R2 model)	$2J^q$ (lattice [40])
u	0.37	0.58	0.74 ± 0.12
d	0.20	−0.06	−0.08 ± 0.08
s	0.04	0.04	
$u + d + s$	0.61	0.56	0.66 ± 0.14

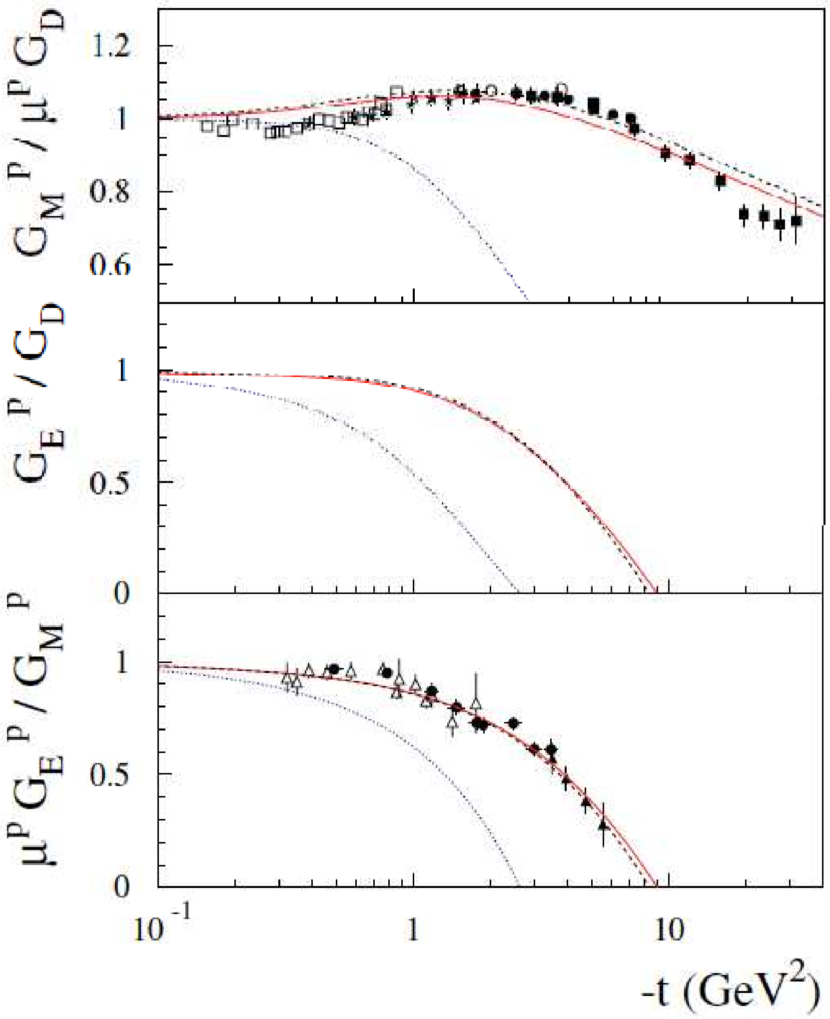

pQCD, I

- Based on dimensional scaling laws for high-Q^2 exclusive reactions:
  - Brodsky, Farrar, PRD 11, 1309 (1975)
  - Brodsky, Lepage PRL 43, 545 (1979)
- Expect $F_{1p} \sim 1/Q^4$, $F_{2p} \sim 1/Q^6$, as $Q^2 \rightarrow \infty$

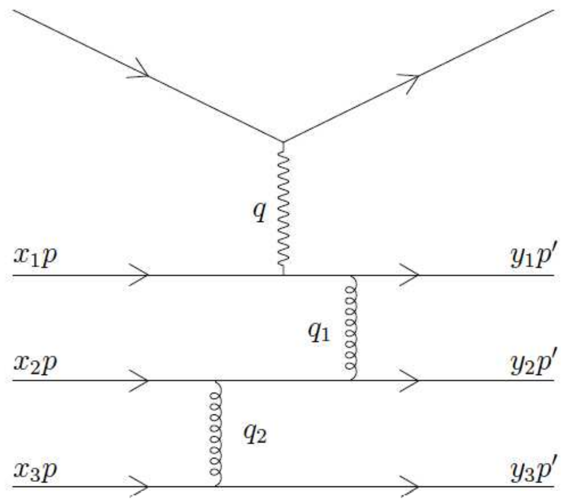

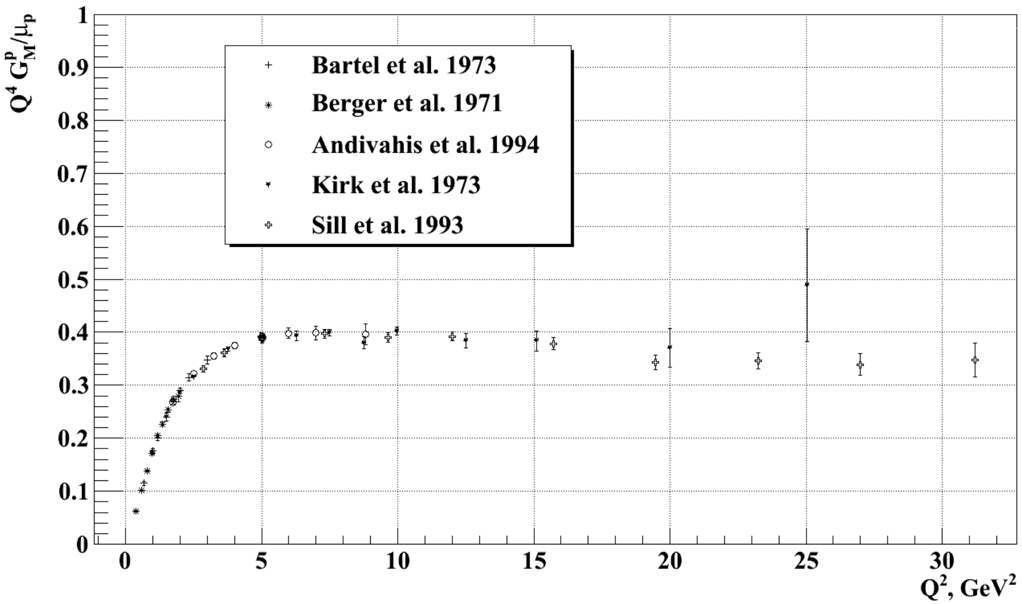

Approximately satisfied by G_{Mp} starting at $Q^2 \approx$ 5-10 GeV^2

pQCD, II

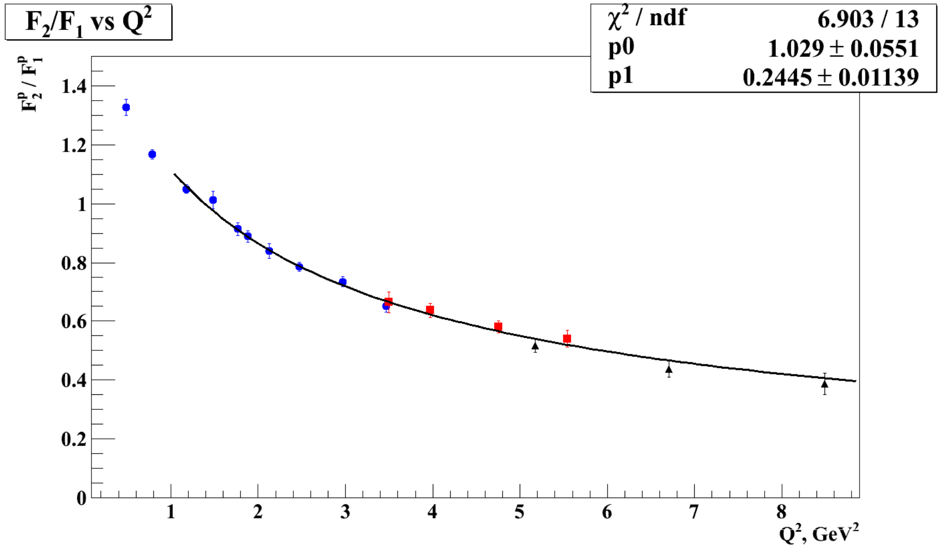

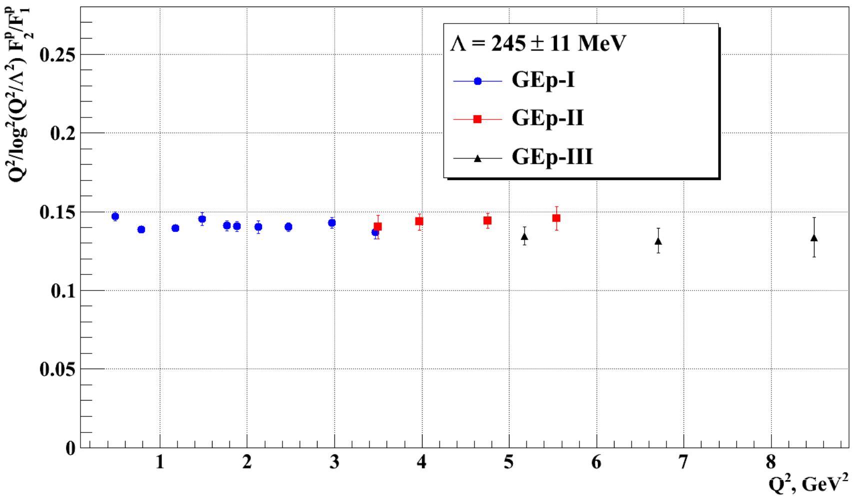

- Belitsky, Ji, Yuan, PRL 91, 092003 (2003)
- pQCD analysis of Pauli form factor F_2
- Subleading-twist component of light cone nucleon D. A. leads to logarithmic modification of asymptotic scaling of F_2 relative to F_1

- Proton data for the ***ratio*** F_2/F_1 well described by this modified scaling
- Necessary, but not sufficient condition for validity of pQCD form factor description
- $$Q^2 \frac{F_2}{F_1} \propto \ln^2\left(\frac{Q^2}{\Lambda^2}\right)$$

pQCD, III

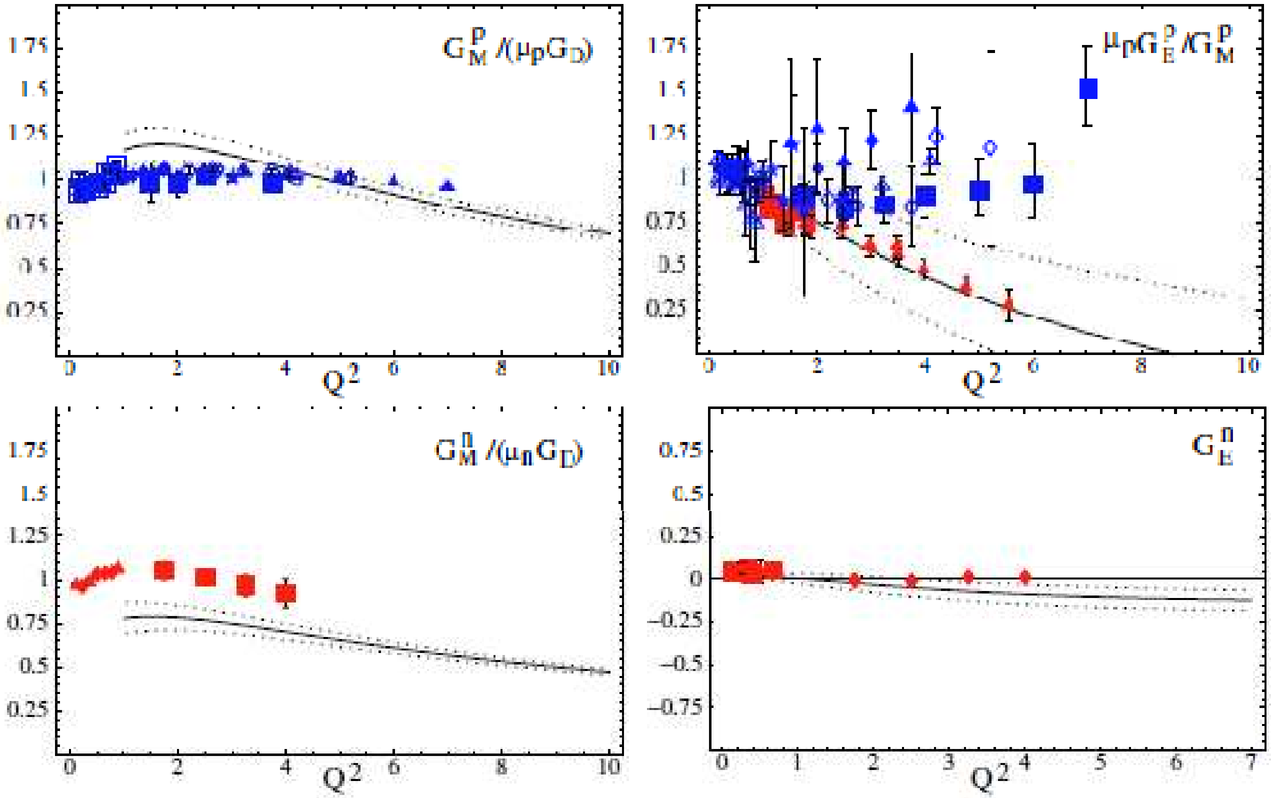

Light cone sum rule calculation of nucleon form factors: Braun, Lenz, and Wittmann, PRD 73, 094019 (2006)

Dyson-Schwinger/Faddeev/q(qq)

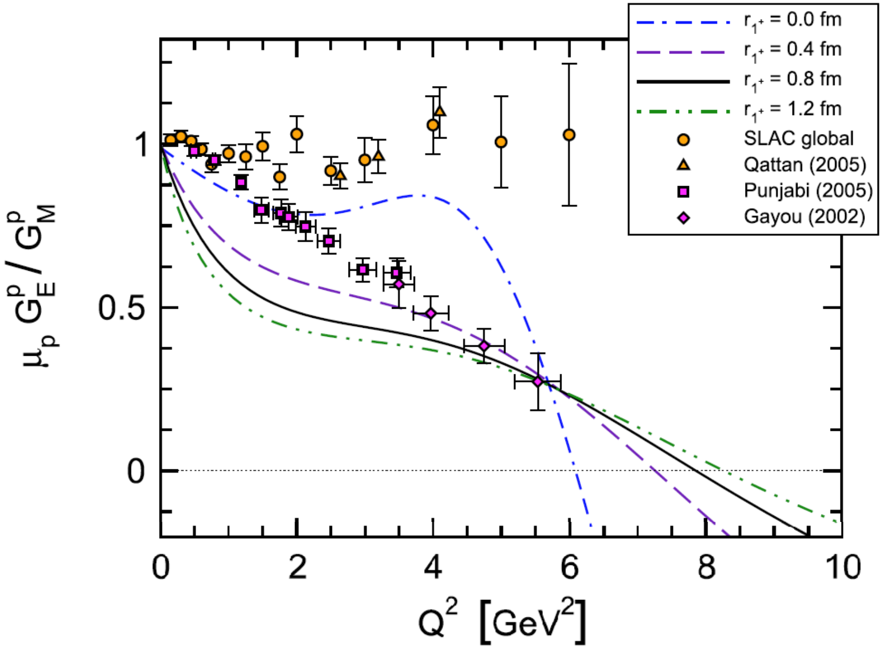

Dressed-quark core contribution to R_p for different diquark radii

- Cloet et al., Few Body Systems, 46, 1 (2009)
- Dressed quarks are fundamental degrees of freedom
- diquark correlations
- Solution of Poincare-covariant Faddeev equations based on rainbow-ladder truncation of DSEs of QCD
- photon-nucleon vertex depends on a single parameter: diquark charge radius
- G_{Ep} and G_{En} both possess a zero

Transverse Densities, I

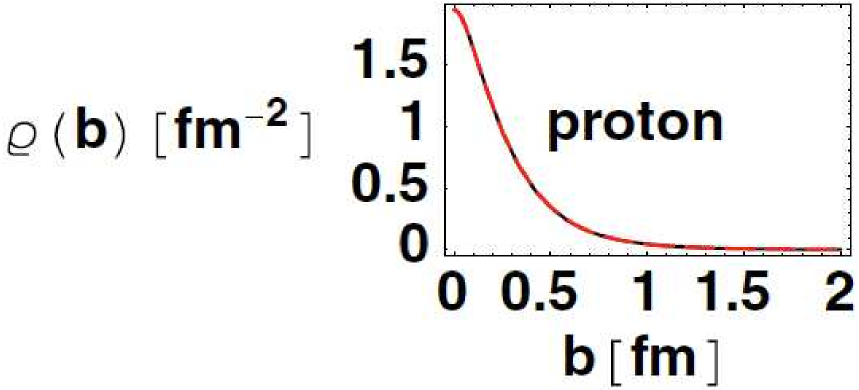

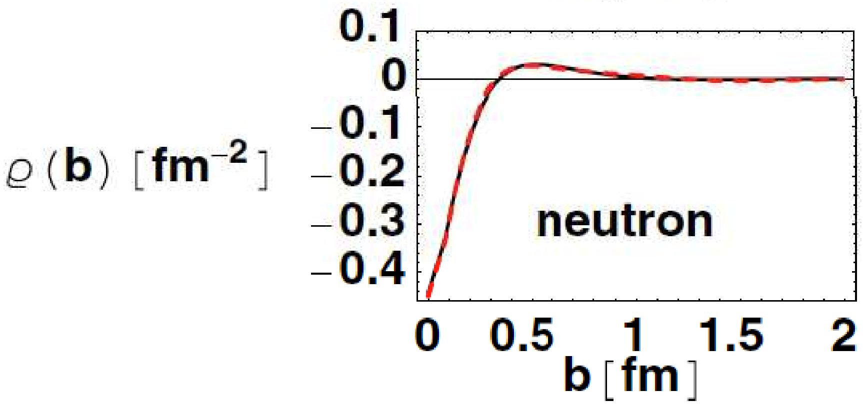

- Burkardt, Int. J. Mod. Phys. A 18, 173 (2003)—GPDs related to impact-parameter distributions:

$$q(x, \mathbf{b}) = \int \frac{d^2q}{(2\pi)^2} e^{i\mathbf{q}\cdot\mathbf{b}} H_q(x, t = -\mathbf{q}^2),$$

- Miller, PRL 99, 112001 (2007)—model-independent infinite-momentum frame transverse charge density from 2D Fourier transform of F_{1p}
- Miller, Piasetzky, Ron, PRL 101, 082002 (2008)—model-independent magnetization density from F_{2p}

$$\rho(b) \equiv \sum_q e_q \int dx q(x, \mathbf{b}) = \int \frac{d^2q}{(2\pi)^2} F_1(Q^2 = \mathbf{q}^2) e^{i\mathbf{q}\cdot\mathbf{b}}. \qquad \rho_M(b) = \int \frac{d^2q}{(2\pi)^2} F_2(t = -\mathbf{q}^2) e^{i\mathbf{q}\cdot\mathbf{b}}.$$

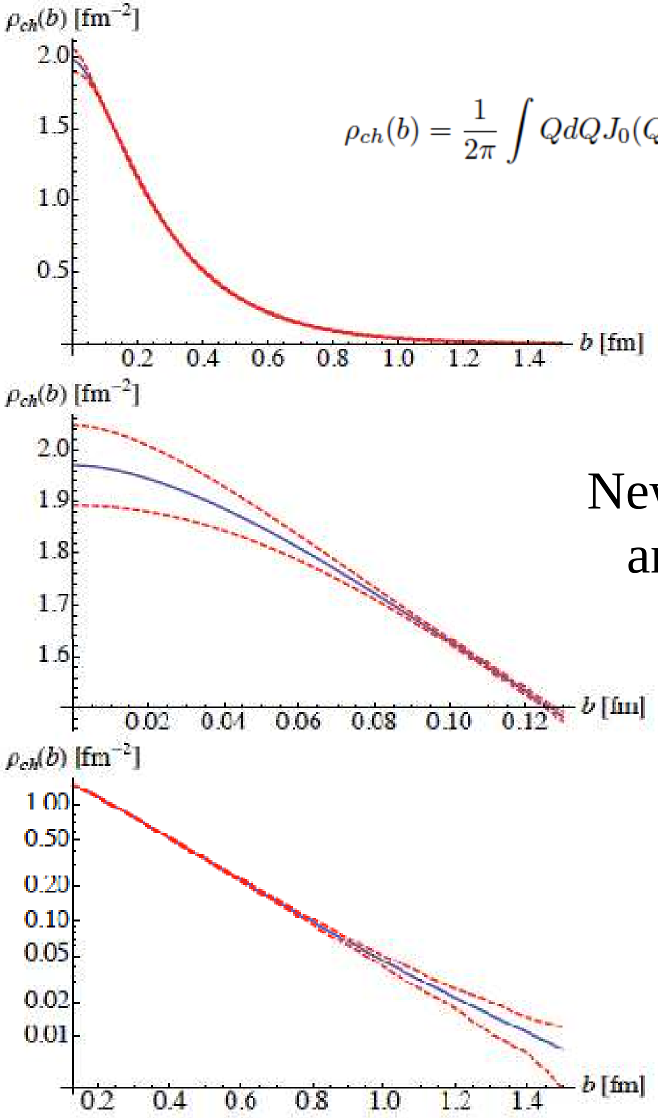

FIG. 7: (Color online) ρ_{ch} (solid, blue) (with error bands (short dashed, red)).

New transverse density analysis of FF data: Miller et al: arxiv:1010.3629

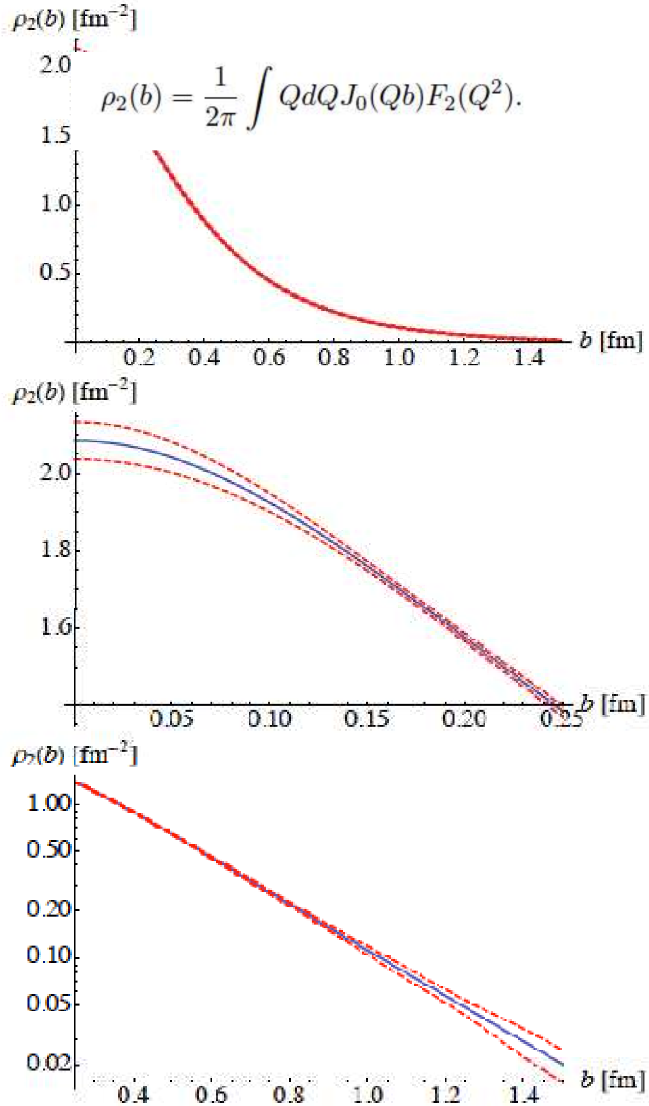

FIG. 8: (Color online) ρ_2, with error bands

Covariant Spectator Model

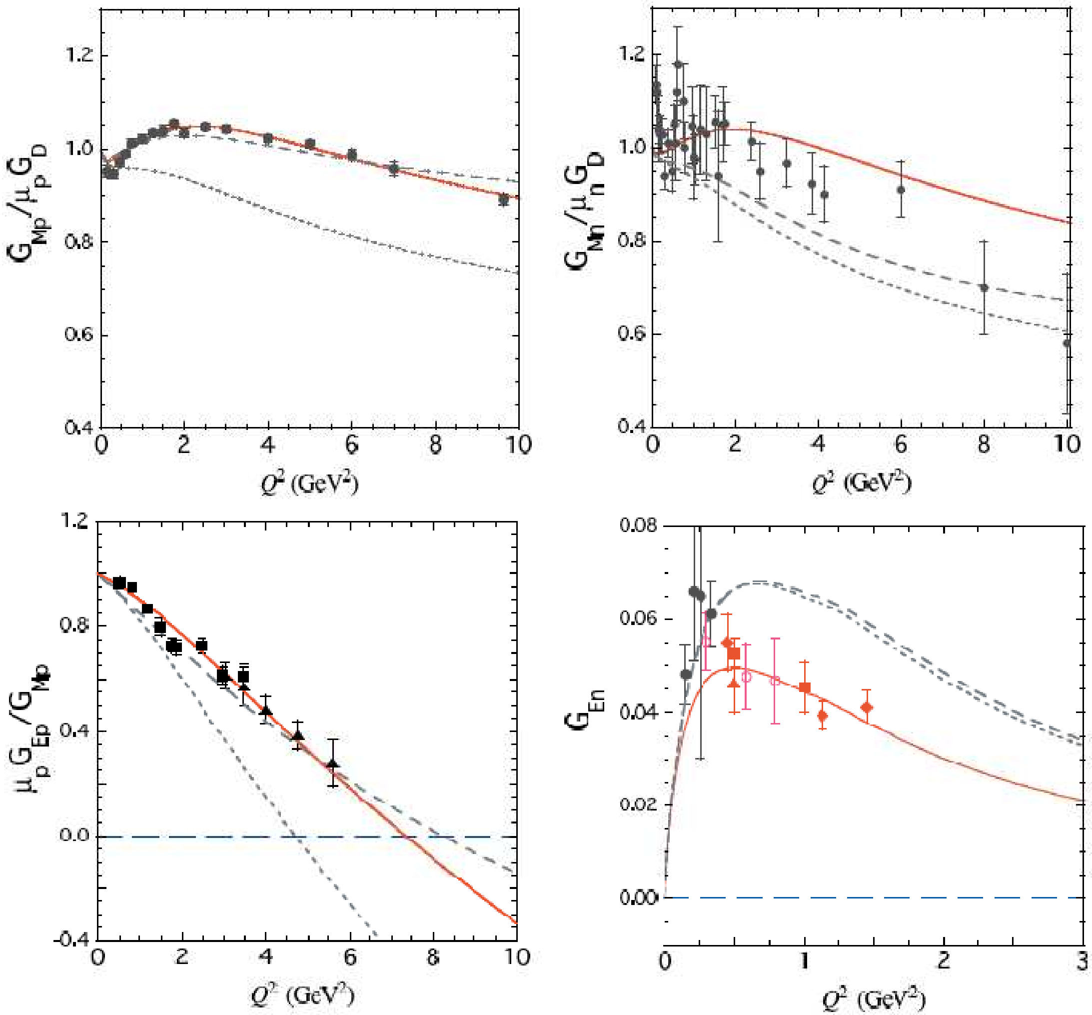

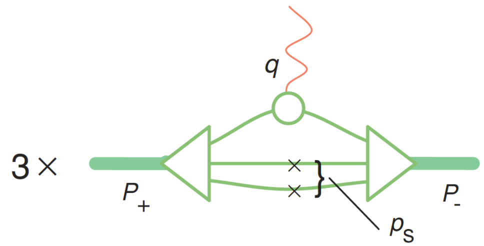

- Gross and Agbakpe, PRC 73, 015203 (2006)
- Also Gross, Ramalho, and Peña, PRC 77, 015202 (2008)
- Model nucleon as bound state of three dressed, valence constituent quarks
- Covariant spectator "diquark" on shell

Theory Overview—TPEX

Radiative Corrections and TPEX in elastic ep→ep

- “Standard” QED radiative corrections to ep cross section data at lowest order in α include:
  - Vertex corrections
  - Vacuum polarization
  - Self-energy
  - Bremsstrahlung
- Two-photon exchange (TPEX) process where both photons are “hard” previously neglected
  - **Cannot be calculated model-independently**
  - **Have been shown to partially resolve the discrepancy between L/T and polarization data for G_{Ep}**

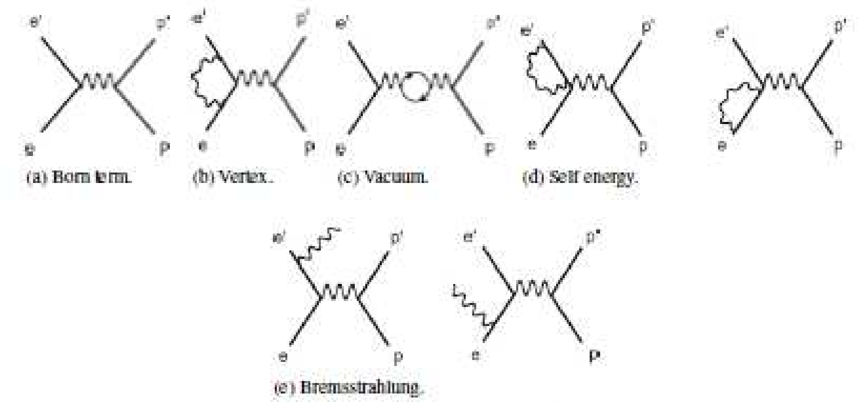

Fig. 24. Born term and lowest order radiative correction graphs for the electron in elastic *ep*.

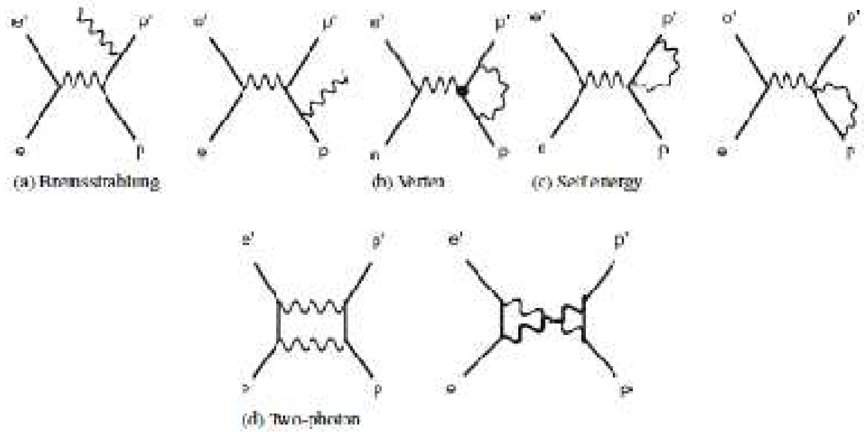

Fig. 25. Lowest order radiative correction for the proton side in elastic *ep* scattering.

Formalism for elastic ep with TPEX

$$
\begin{aligned}
P_t &= -\sqrt{\frac{2\epsilon(1-\epsilon)}{\tau}}\,\frac{h}{\sigma_r}\Big[G_E G_M + G_M \Re\Big(\delta\tilde{G}_E + \frac{\nu}{M^2}\tilde{F}_3\Big) \\
&\quad + G_E \Re(\delta\tilde{G}_M) + \mathcal{O}(e^4)\Big] \\
P_\ell &= h\frac{\sqrt{1-\epsilon^2}}{\sigma_r}\Big[G_M^2 + 2G_M\Re\Big(\delta\tilde{G}_M + \frac{\nu}{M^2}\frac{\epsilon}{1+\epsilon}\tilde{F}_3\Big) \\
&\quad + \mathcal{O}(e^4)\Big] \\
\sigma_r &= G_M^2 + \frac{\epsilon}{\tau}G_E^2 + \frac{2\epsilon}{\tau}G_E\Re\Big(\delta\tilde{G}_E + \frac{\nu}{M^2}\tilde{F}_3\Big) \\
&\quad + 2G_M\Re\Big(\delta\tilde{G}_M + \frac{\epsilon\nu}{M^2}\tilde{F}_3\Big) + \mathcal{O}(e^4) \\
R &= \frac{G_E}{G_M}\Re\Big[1 - \frac{\delta\tilde{G}_M}{G_M} + \frac{\delta\tilde{G}_E}{G_E} + \frac{\nu\tilde{F}_3}{M^2} \\
&\quad \times\Big(\frac{1}{G_E} - \frac{2\epsilon}{1+\epsilon}\frac{1}{G_M}\Big) + \mathcal{O}(e^4)\Big] \qquad (1)
\end{aligned}
$$

- In the Born approximation (one photon exchange mechanism), elastic ep scattering described by two ***real*** amplitudes (G_E, G_M), functions of Q^2
- With TPEX contribution, we have instead three ***complex*** amplitudes, depend on Q^2, ε

Experimental studies of TPEX

- Beam and target SSAs in elastic ep scattering: Imaginary part of TPEX amplitude (target SSA equivalent to induced recoil polarization in ep scattering)
- e^+p/e^-p cross section ratio—expect few percent deviation from unity
- Non-linearity in the Rosenbluth plot—none yet observed; high precision ep cross section measurements in Hall C (experiment E05-017), analysis in progress
- ε dependence of R_p recoil polarization—experiment E04-019

TPEX—Hadronic Model

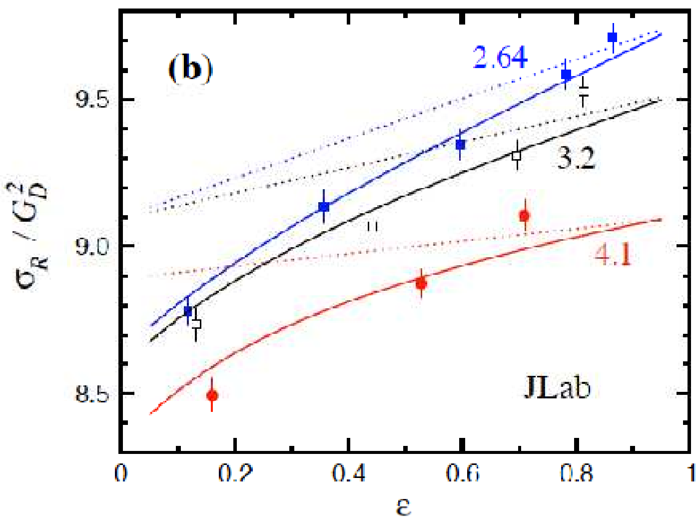

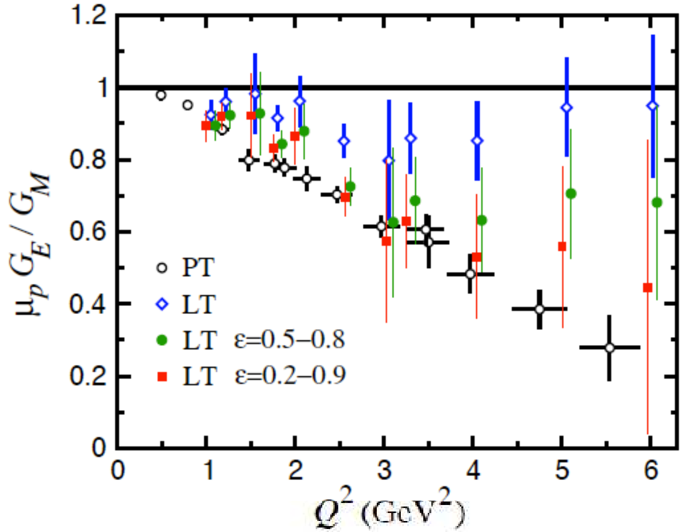

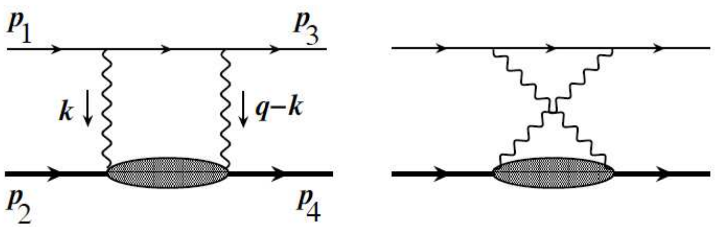

FIG. 1: Two-photon exchange box and crossed box diagrams for elastic electron–proton scattering.

- Blunden, Melnitchouk, Tjon, PRC 72, 034612 (2005): TPEX corrections with N intermediate state;

- Nucleon form factors included at each photon-nucleon vertex
- Correction to σ_R of order few percent, but strongly ε dependent
- Partially reconciles LT/PT results
- Predicts several % increase in R extracted from P_t/P_l ratio at low ε relative to ε=1

TPEX—Partonic Model

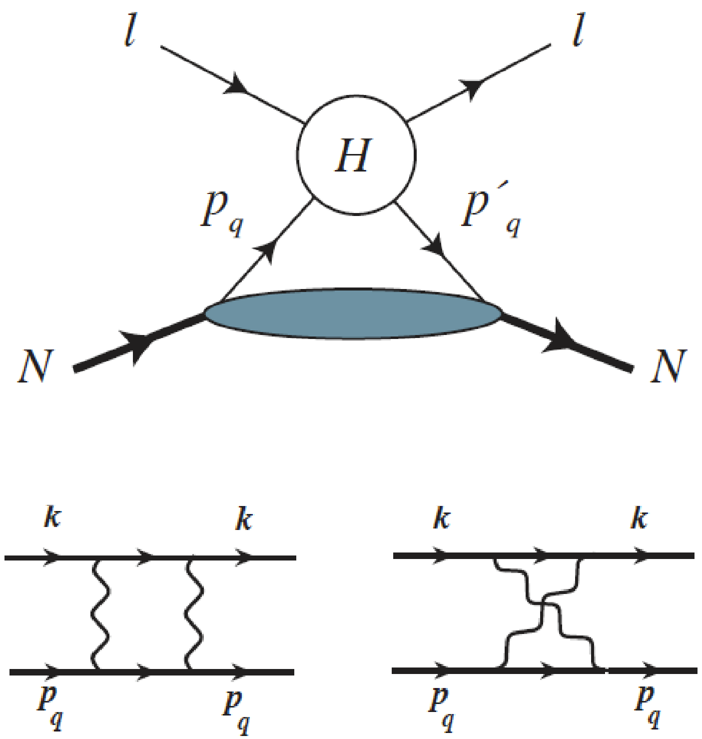

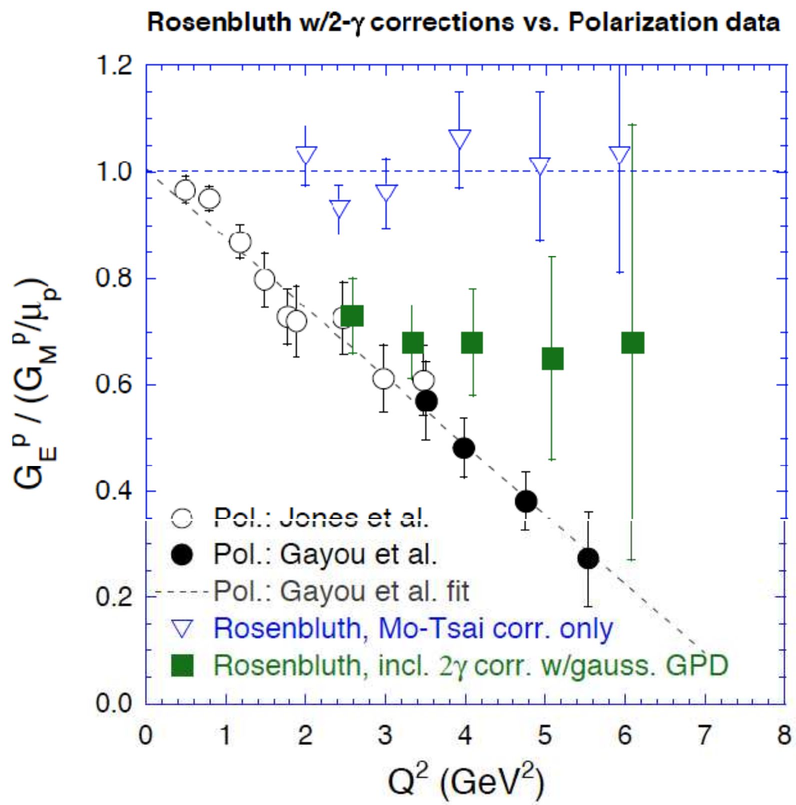

- Afanasev, Brodsky, Carlson, Chen, and Vanderhaeghen, PRD 72, 013008 (2005): TPEX correction related to GPDs in handbag mechanism, valid at "large" s, u, -t
- Predicts a strong decrease of Pt/Pl at low ε

Structure Function Method

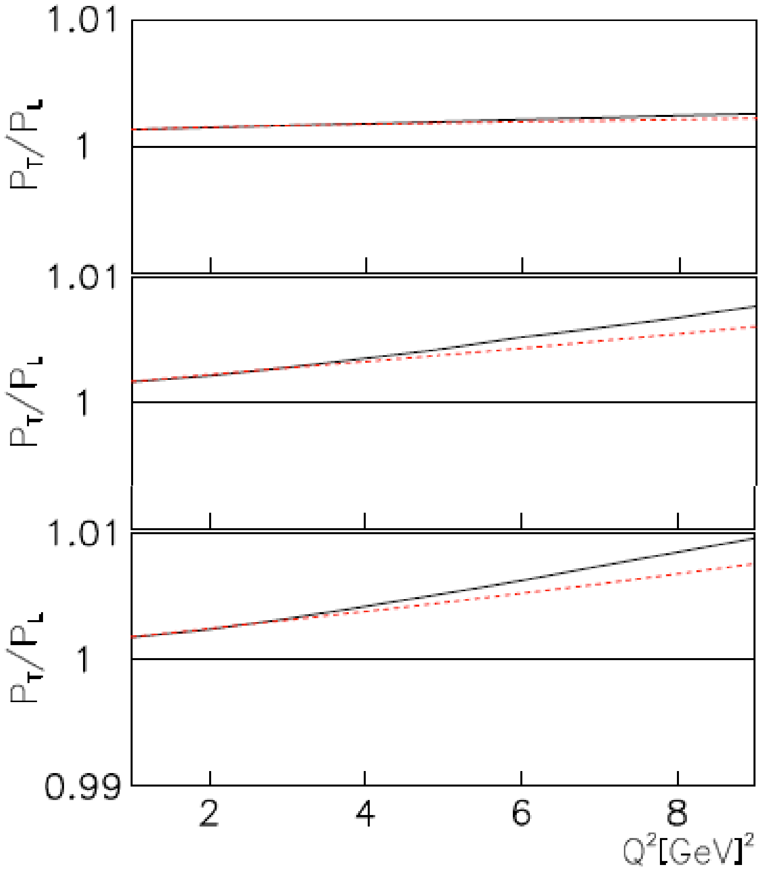

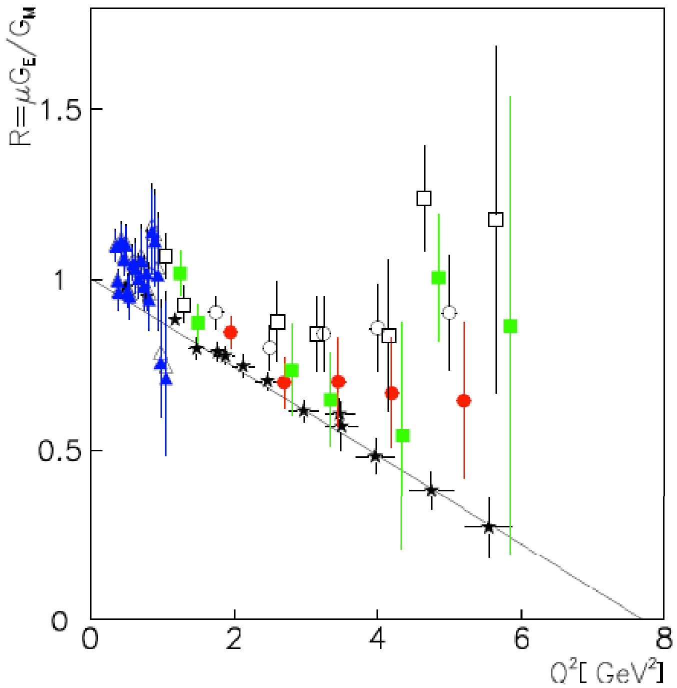

- Bystritskiy et al. PRC 75, 015207 (2007)
- Calculation of RC to elastic ep cross section using electron SF approach
- Largely reconciles discrepancy
- Very small effect predicted for PT results, in agreement with E04-019 measurements

E99-007 Reanalysis

Consistency of High-Q^2 G_{Ep} Data?

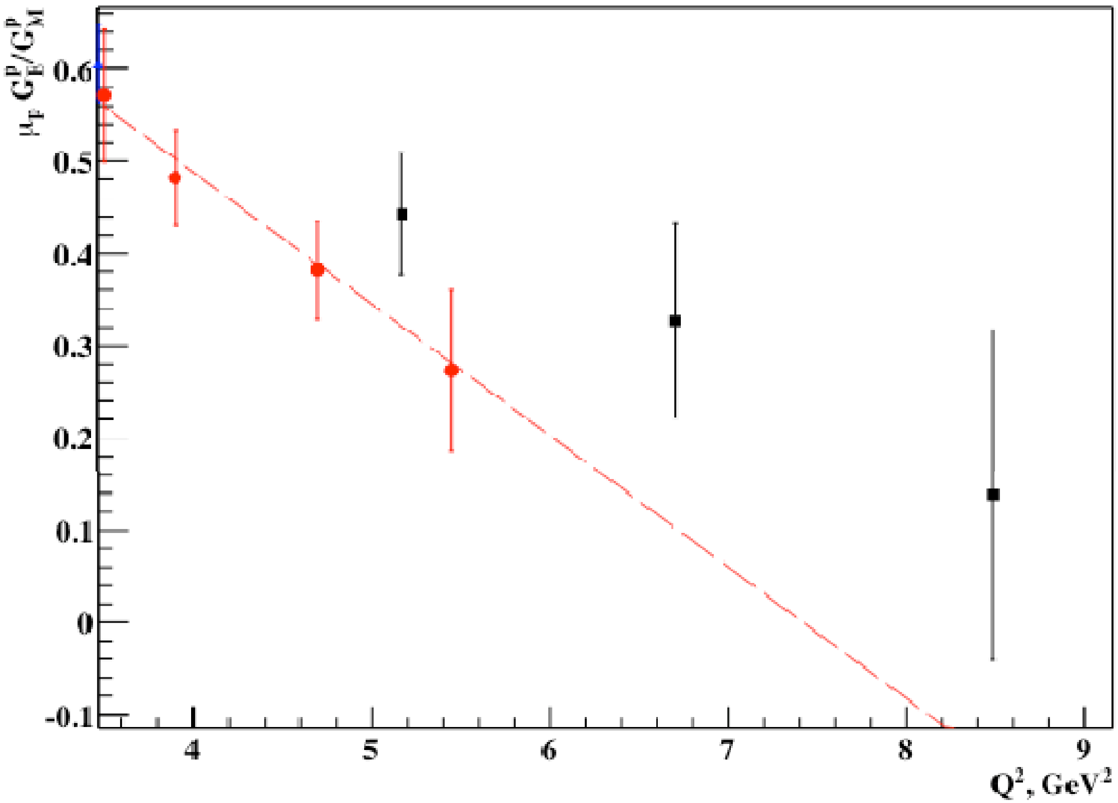

Comparison of Gayou et al. (GEp-II) and GEp-III data, and linear fit to GEp-I+II data

- Previous recoil polarization data well described by a straight line for $0.4<Q^2<5.6$ GeV^2
- Each data point from GEp-III at least 1.5σ above linear fit to previous data
- No compelling reason for linear decrease to continue
- Probability of GEp-III data with respect to previous straight-line fit only ~1.4%
- **Reanalysis of GEp-II data to investigate systematic difference between two experiments**

Elastic event selection, GEp-II

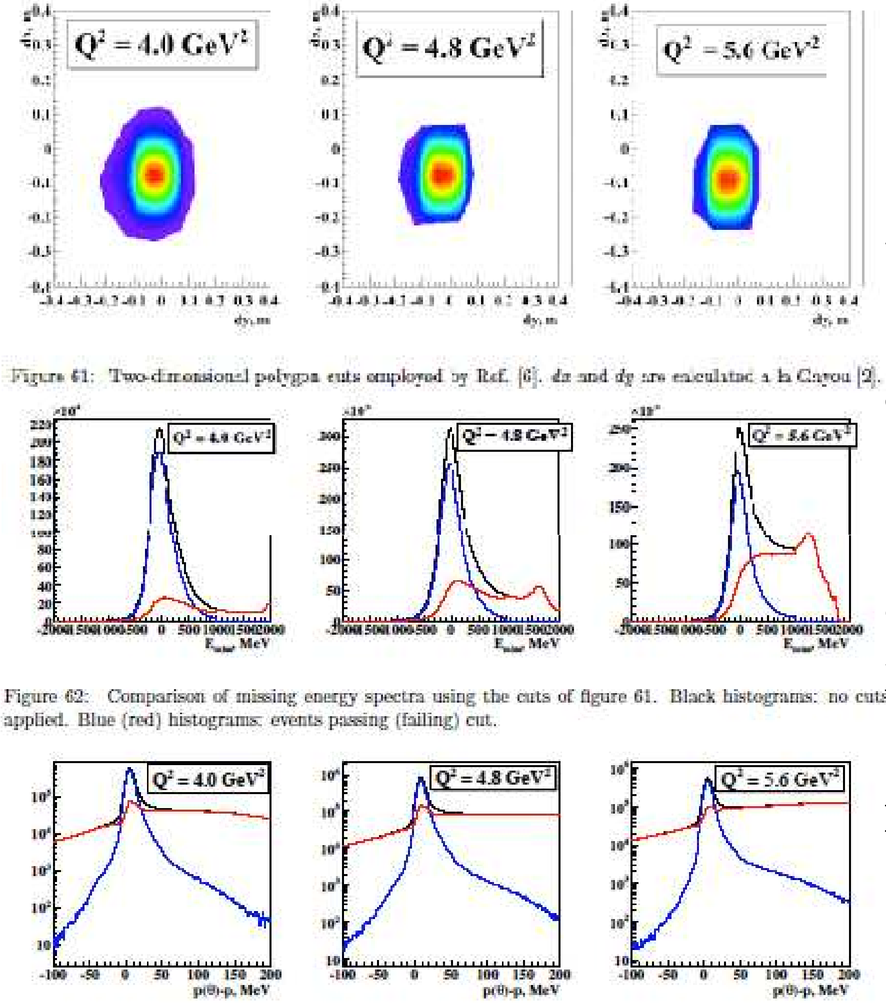

Figure 61: Two-dimensional polygon cuts employed by Ref. [6]. dx and dy are calculated a la Cayou [2].

Figure 62: Comparison of missing energy spectra using the cuts of figure 61. Black histograms: no cuts applied. Blue (red) histograms: events passing (failing) cut.

Figure 63: Comparison of "p_{miss}" spectra using the cuts of figure 61. Black histograms: no cuts applied. Blue (red) histograms: events passing (failing) cut.

69

- GEp-II measurements at Q^2=4.0, 4.8, and 5.6 GeV^2 used a lead-glass calorimeter similar to GEp-III; nearly identical method for elastic event selection
- **No cut was applied to the proton angle-momentum correlation in the original GEp-II analysis**
- Tail of p(θ)-p distribution was interpreted as ep radiative tail; these events were included in the original analysis
- In reality, this tail is a mixture of ep radiative tail and π^0 photoproduction
    - **GEp-III cut suppresses rad. tail completely**
    - **GEp-II cut allows some rad. tail events**
- Contamination/polarization of background affects FF ratio extraction

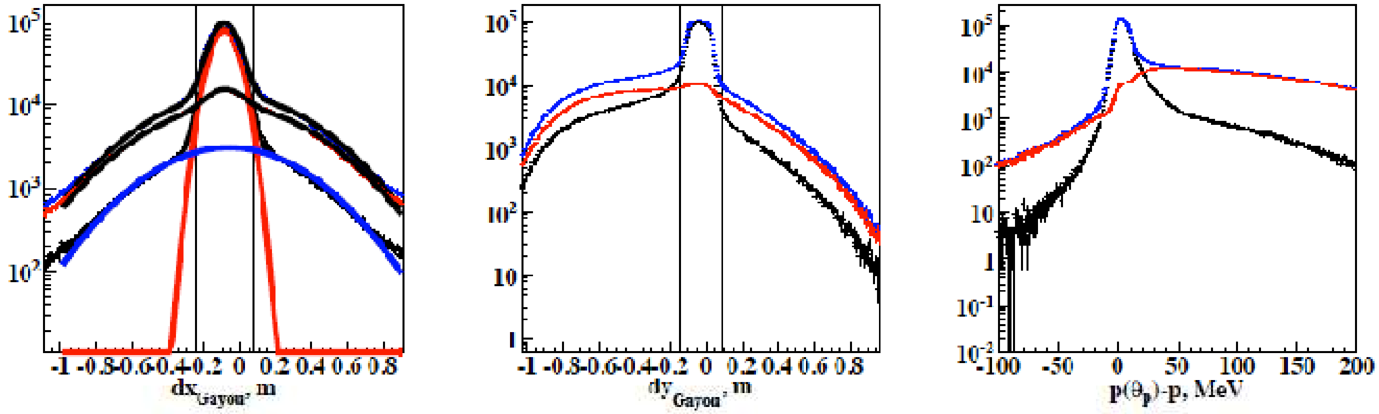

Figure 2.5: Background estimation, $Q^2 - 5.6$ GeV^2, part 1, Gayou cuts, no p_{miss} cut.

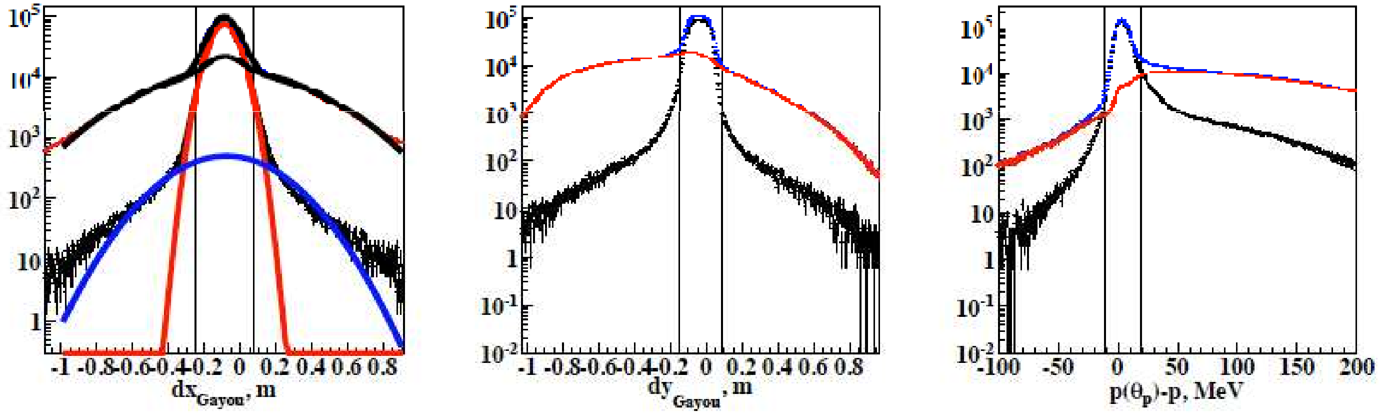

Figure 2.6: Background estimation, $Q^2 = 5.6$ GeV^2, part 1, Gayou cuts, p_{miss} cut.

Comparison of background, with and without p(θ)-p cut, Q^2=5.6 GeV^2

Effect of background on GEp-II data

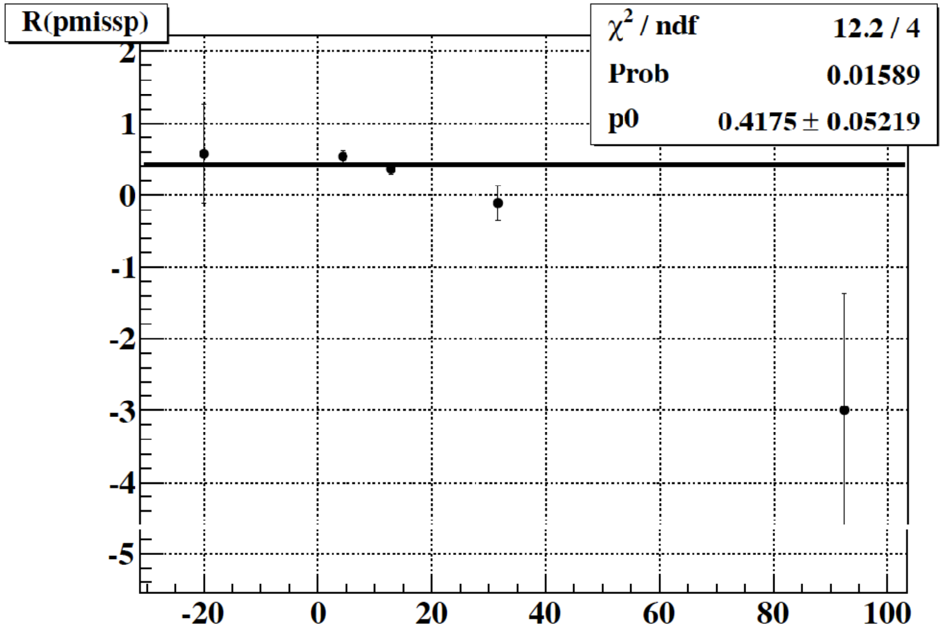

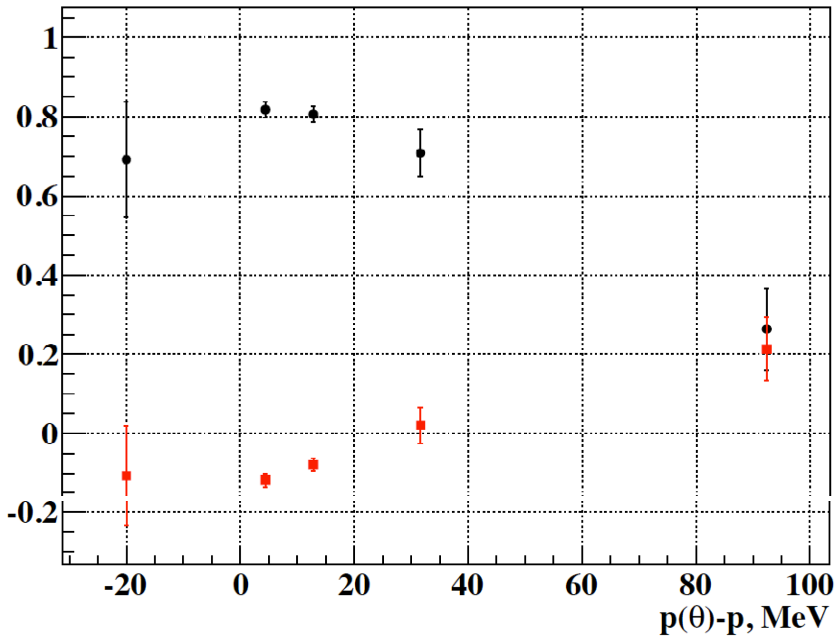

Form factor ratio; $R=\mu G_E/G_M$ vs. $p(\theta)$-p, Q^2=4.8 GeV^2

P_l, (black circles), P_t (red squares) vs. $p(\theta)$-p, Q^2=4.8 GeV^2

- π^0 background transverse polarization is large, opposite to elastic ep.
- Longitudinal polarization same sign, but smaller
- Net effect is a strong negative pull on R due to background; leads to a positive correction

Preliminary Results of GEp-II Reanalysis

- **New analysis identical in all respects to original except for elastic event selection cuts.**
- Only additional cut is “p_{miss}”; i.e., p(θ)-p
- R increases for all three Q^2, largest increase for Q^2 = 4.8 GeV^2
- Improved consistency of high-Q^2 G_{Ep} data
- No background subtraction applied yet, corrections expected at ΔR ≈ +.01 or less

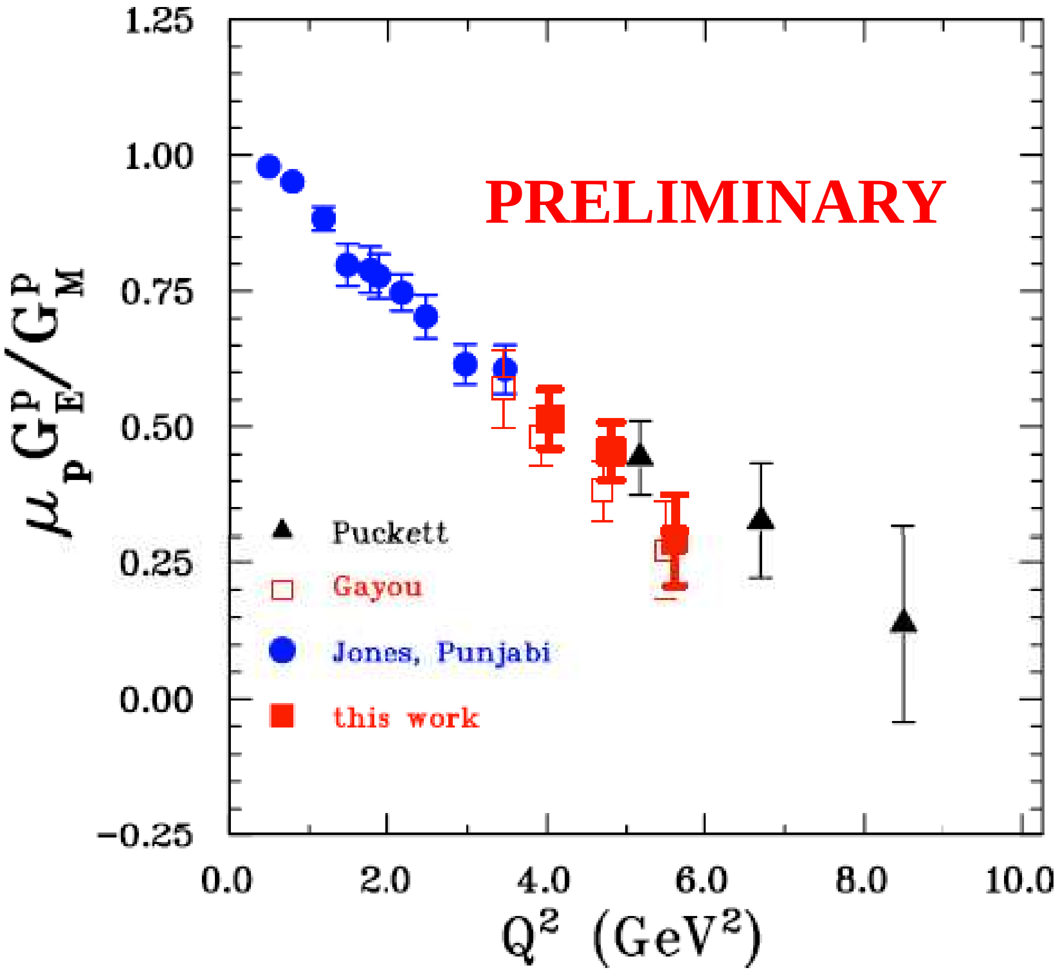

R_p recoil polarization data, GEp-II reanalysis

Statistical Impact of E04-108

Statistical Impact of GEp-III

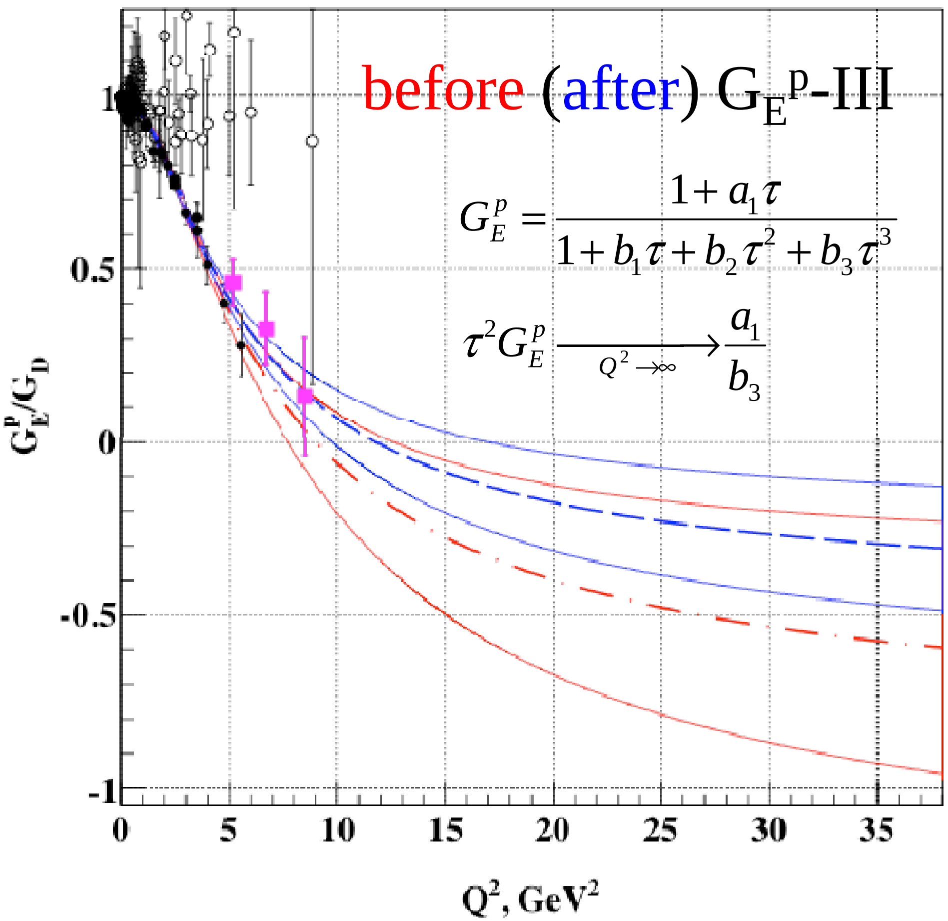

- Global fit of G_E^p and G_M^p using Kelly parametrization: PRC 70, 068202 (2004)
- Including GEp-III data pushes zero crossing from ~9 to ~12 GeV^2, reduces uncertainty in asymptotic G_E^p/G_D by a factor of more than 2.
- Details of global analysis to appear in proceedings of 4th Workshop on Exclusive Reactions at High Momentum Transfer; arxiv:1008.0855

Global Fit and G_M^p

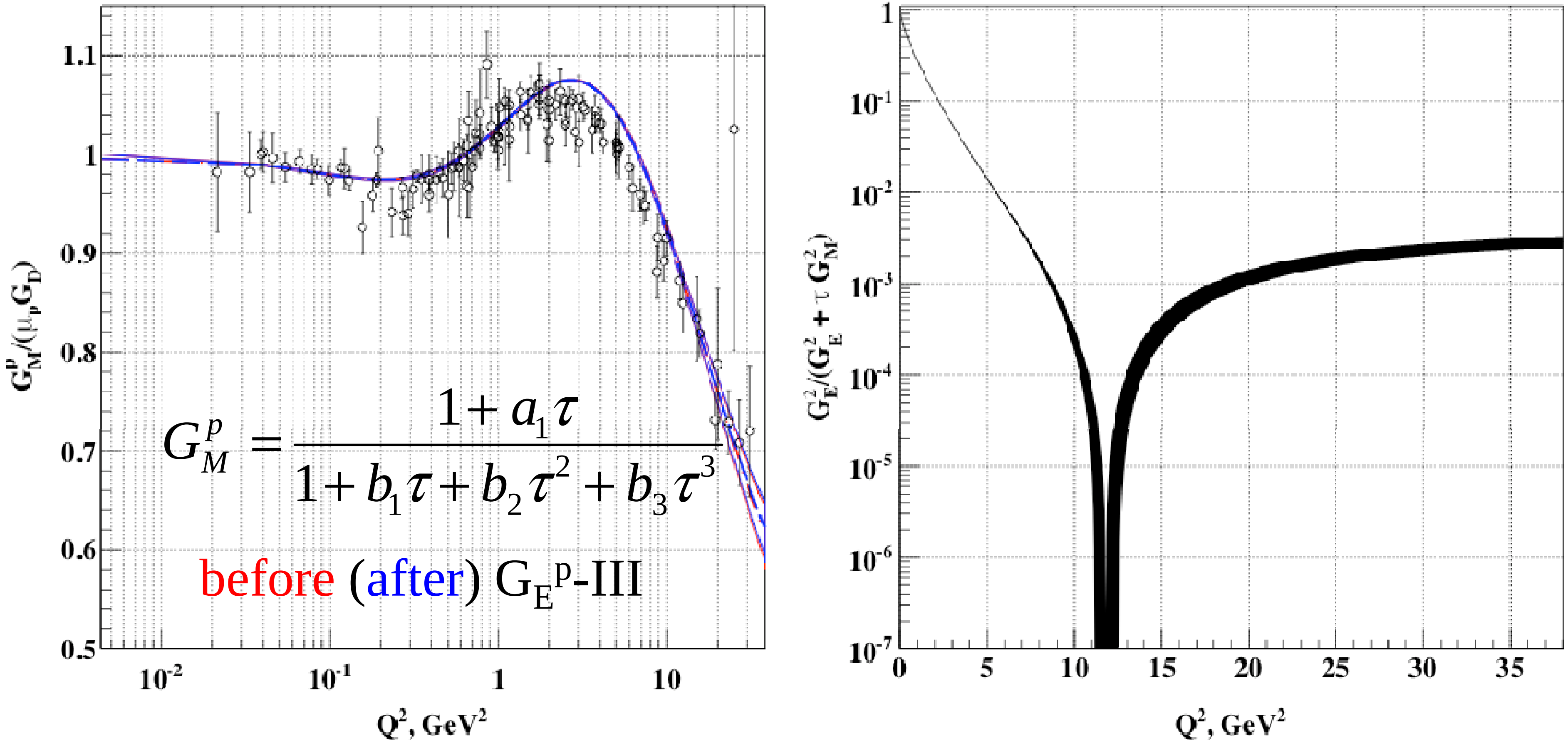

• Global analysis using constraint on R from polarization data brings a small systematic increase in G_M^p, consistent with other global analyses; e.g. Arrington, Melnitchouk, Tjon, PRC 76, 035205 (2007) (global analysis with TPEX corrections)

Global Fit and F_{1p}/F_{2p}

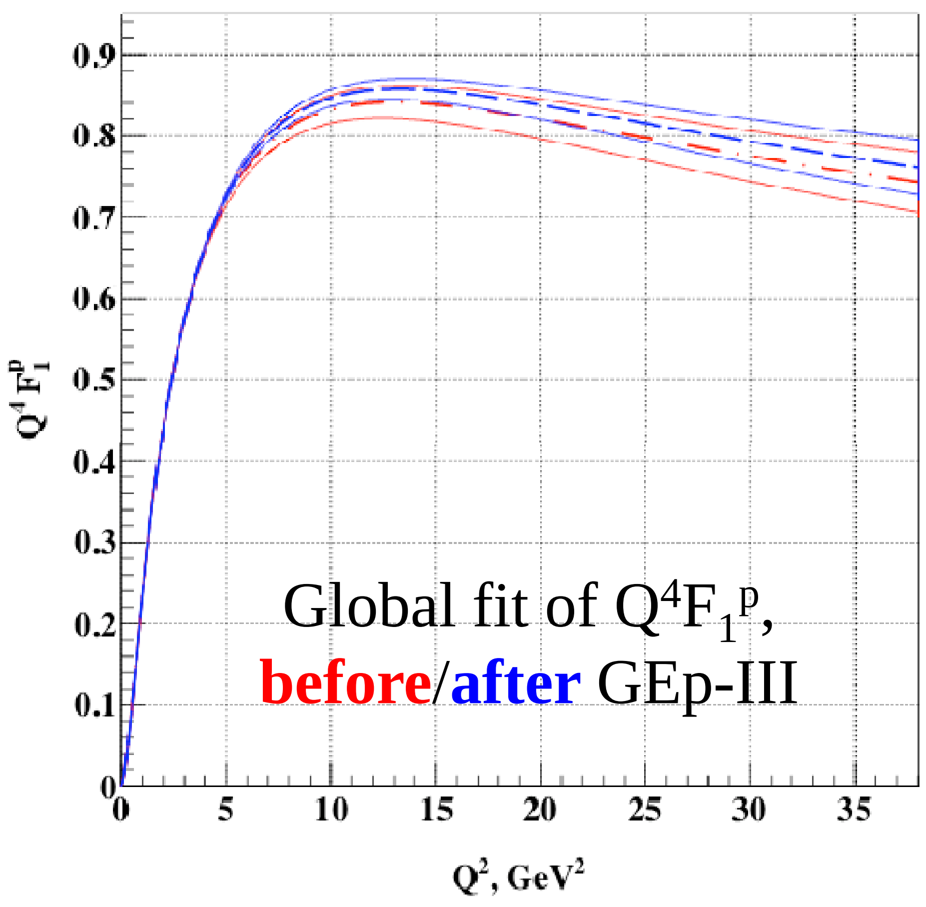

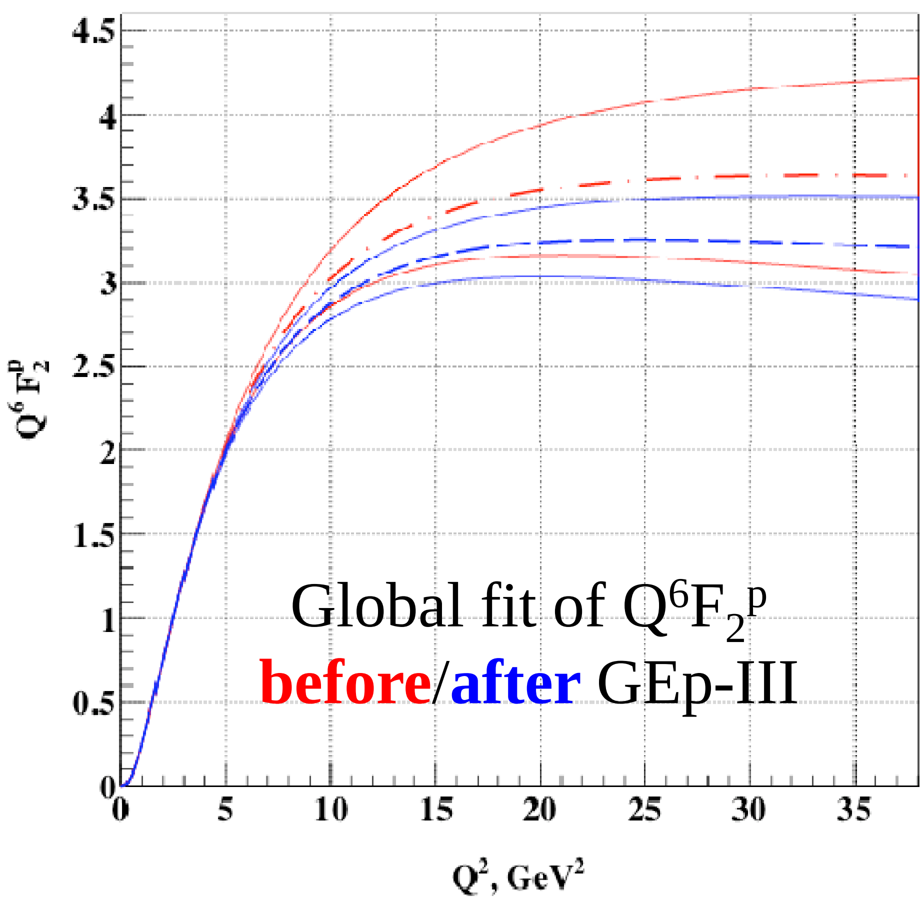

Conclusion

- GEp-III results published: **PRL 104, 242301(2010); arxiv:1005.3419**
- Extended recoil polarization data to Q^2 = 8.5 GeV^2
- Significant new constraints on high-Q^2 behavior of F. F. models, GPD moments, transverse charge and magnetization densities, etc.
- GEp-2γ results nearly final; submission to PRL expected in December
- E99-007 reanalysis nearly final—new results much more consistent with E04-108; we will publish, probably in Phys. Rev. C, very soon

Future Measurements of GEp/GMp: The JLab 12(11) GeV Upgrade

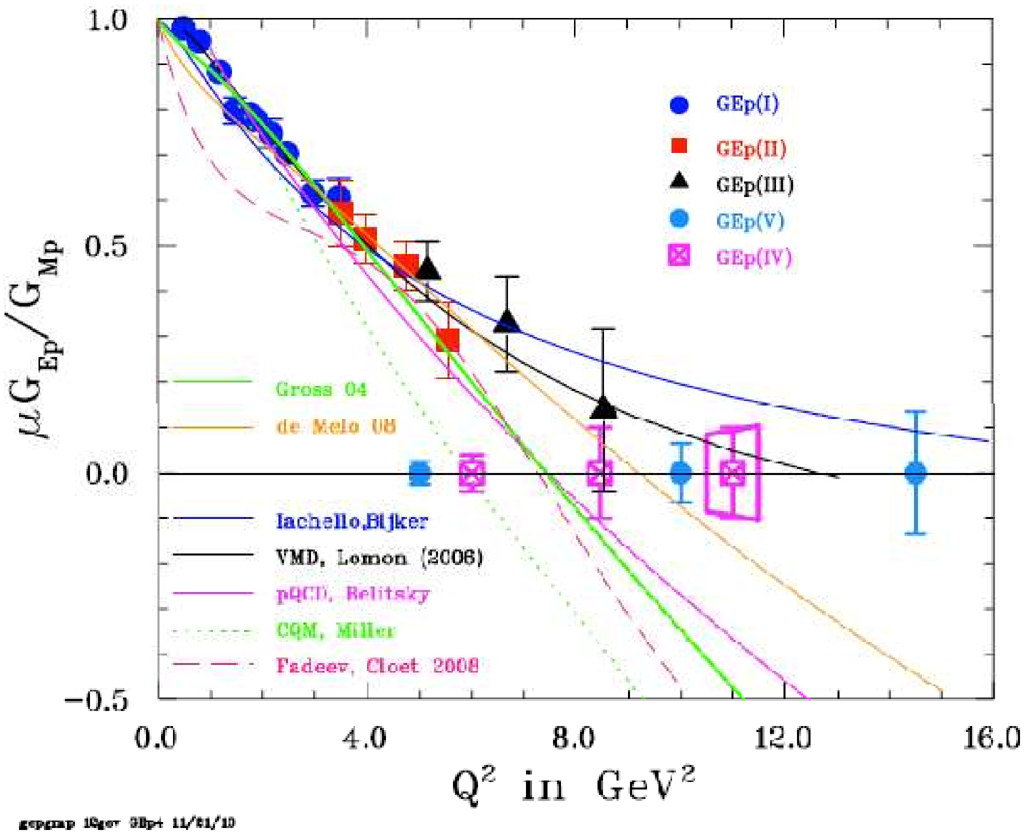

Proton form factors ratio, GEp(5) (E12-07-109)

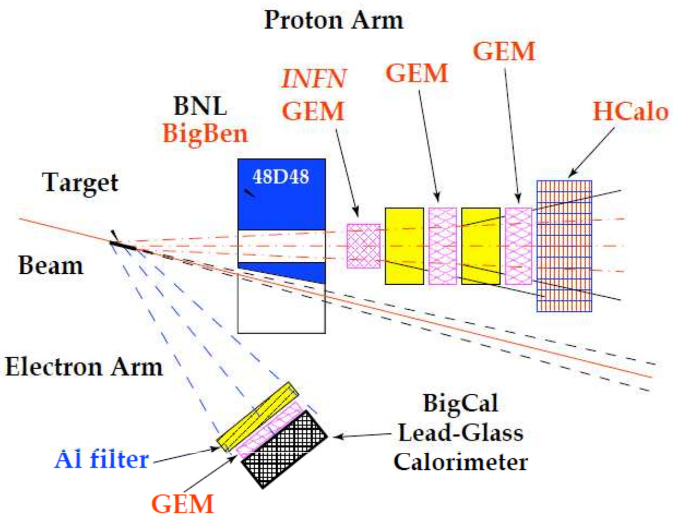

- Large Acceptance measurements to Q^2=15 GeV^2; SBS project (GEp-V)
- HMS+BigCal to Q^2=11 GeV^2 in Hall C (GEp-IV)

GEp-III/GEp-2γ Collaboration

Recoil Polarization Measurements of the Proton Electromagnetic Form Factor Ratio to $Q^2 = 8.5$ GeV^2

A. J. R. Puckett,[1,*] E. J. Brash,[2,3] M. K. Jones,[3] W. Luo,[4] M. Meziane,[5] L. Pentchev,[5] C. F. Perdrisat,[5] V. Punjabi,[6] F. R. Wesselmann,[6] A. Ahmidouch,[7] I. Albayrak,[8] K. A. Aniol,[9] J. Arrington,[10] A. Asaturyan,[11] H. Baghdasaryan,[12] F. Benmokhtar,[13] W. Bertozzi,[1] L. Bimbot,[14] P. Bosted,[3] W. Boeglin,[15] C. Butuceanu,[16] P. Carter,[2] S. Chernenko,[17] E. Christy,[8] M. Commisso,[12] J. C. Cornejo,[9] S. Covrig,[3] S. Danagoulian,[7] A. Daniel,[18] A. Davidenko,[19] D. Day,[12] S. Dhamija,[15] D. Dutta,[20] R. Ent,[3] S. Frullani,[21] H. Fenker,[3] E. Frlez,[12] F. Garibaldi,[21] D. Gaskell,[3] S. Gilad,[1] R. Gilman,[3,22] Y. Goncharenko,[19] K. Hafidi,[10] D. Hamilton,[23] D. W. Higinbotham,[3] W. Hinton,[6] T. Horn,[3] B. Hu,[4] J. Huang,[1] G. M. Huber,[16] E. Jensen,[2] C. Keppel,[8] M. Khandaker,[6] P. King,[18] D. Kirillov,[17] M. Kohl,[8] V. Kravtsov,[19] G. Kumbartzki,[22] Y. Li,[8] V. Mamyan,[12] D. J. Margaziotis,[9] A. Marsh,[2] Y. Matulenko,[19] J. Maxwell,[12] G. Mbianda,[24] D. Meekins,[3] Y. Melnik,[19] J. Miller,[25] A. Mkrtchyan,[11] H. Mkrtchyan,[11] B. Moffit,[1] O. Moreno,[9] J. Mulholland,[12] A. Narayan,[20] S. Nedev,[26] Nuruzzaman,[20] E. Piasetzky,[27] W. Pierce,[2] N. M. Piskunov,[17] Y. Prok,[2] R. D. Ransome,[22] D. S. Razin,[17] P. Reimer,[10] J. Reinhold,[15] O. Rondon,[12] M. Shabestari,[12] A. Shahinyan,[11] K. Shestermanov,[19,†] S. Širca,[28] I. Sitnik,[17] L. Smykov,[17,†] G. Smith,[3] L. Solovyev,[19] P. Solvignon,[10] R. Subedi,[12] E. Tomasi-Gustafsson,[14,29] A. Vasiliev,[19] M. Veilleux,[2] B. B. Wojtsekhowski,[3] S. Wood,[3] Z. Ye,[8] Y. Zanevsky,[17] X. Zhang,[4] Y. Zhang,[4] X. Zheng,[12] and L. Zhu[1]

Institutions

[1] *Massachusetts Institute of Technology, Cambridge, MA 02139*
[2] *Christopher Newport University, Newport News, VA 23606*
[3] *Thomas Jefferson National Accelerator Facility, Newport News, VA 23606*
[4] *Lanzhou University, Lanzhou 730000, Gansu, Peoples Republic of China*
[5] *College of William and Mary, Williamsburg, VA 23187*
[6] *Norfolk State University, Norfolk, VA 23504*
[7] *North Carolina A&T State University, Greensboro, NC 27411*
[8] *Hampton University, Hampton, VA 23668*
[9] *California State University Los Angeles, Los Angeles, CA 90032*
[10] *Argonne National Laboratory, Argonne, IL, 60439*
[11] *Yerevan Physics Institute, Yerevan 375036, Armenia*
[12] *University of Virginia, Charlottesville, VA 22904*
[13] *Carnegie Mellon University, Pittsburgh, PA 15213*
[14] *Institut de Physique Nucléaire, CNRS/IN2P3 and Université Paris-Sud, France*
[15] *Florida International University, Miami, FL 33199*
[16] *University of Regina, Regina, SK S4S OA2, Canada*
[17] *JINR-LHE, Dubna, Moscow Region, Russia 141980*
[18] *Ohio University, Athens, Ohio 45701*
[19] *IHEP, Protvino, Moscow Region, Russia 142284*
[20] *Mississippi State University, Mississippi, MS 39762*
[21] *INFN, Sezione Sanità and Istituto Superiore di Sanità, 00161 Rome, Italy*
[22] *Rutgers, The State University of New Jersey, Piscataway, NJ 08855*
[23] *University of Glasgow, Glasgow G12 8QQ, Scotland UK*
[24] *University of Witwatersrand, Johannesburg, South Africa*
[25] *University of Maryland, College Park, MD 20742*
[26] *University of Chemical Technology and Metallurgy, Sofia, Bulgaria*
[27] *University of Tel Aviv, Tel Aviv, Israel*
[28] *University of Ljubljana, SI-1000 Ljubljana, Slovenia*
[29] *DSM, IRFU, SPhN, Saclay, 91191 Gif-sur-Yvette, France*

Backup Slides

FPP Reconstruction

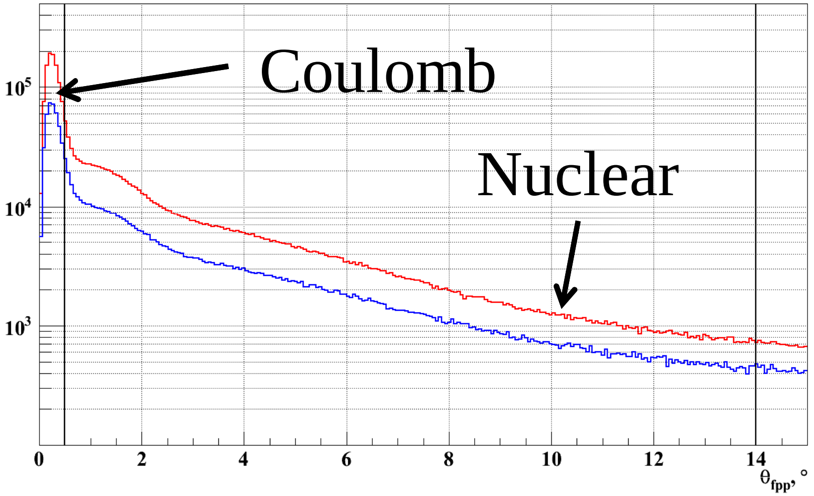

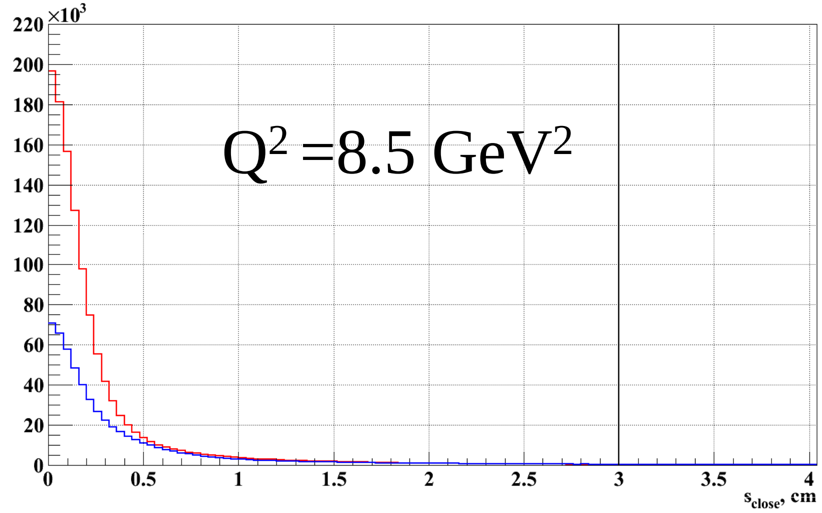

- FPP1 (FPP2) event distributions:
  - Polar angle θ (top left)
  - Closest approach distance s_{close} (top right)
  - θ vs point of closest approach z_{close} (bottom right)
- Black lines represent analysis cuts

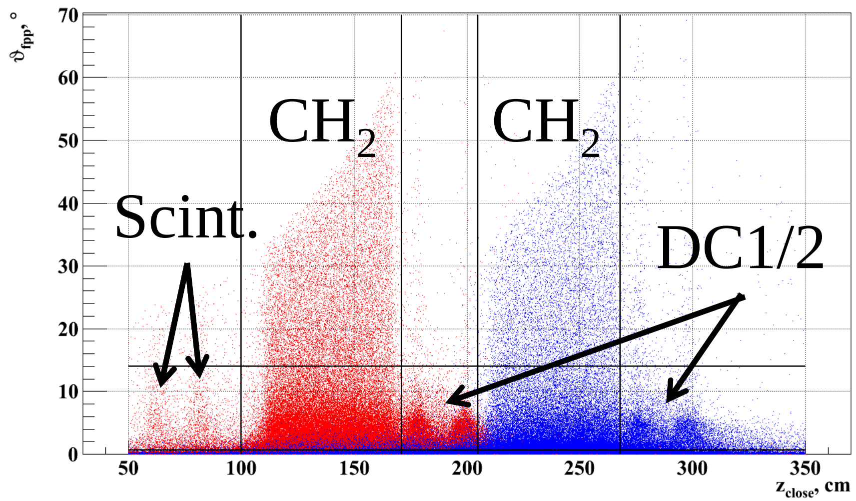

False Asymmetries

- Helicity-independent false/instrumental asymmetries caused by:
  - FPP acceptance/efficiency
  - φ misreconstruction:
    - Misalignment (1φ)
    - xy resolution asymmetry (2φ)
- θ-dependent (bottom right)
- Cancelled by helicity reversal to first order
- Second-order effects small
- ***Measured*** using sum distribution and ***corrected*** in analysis

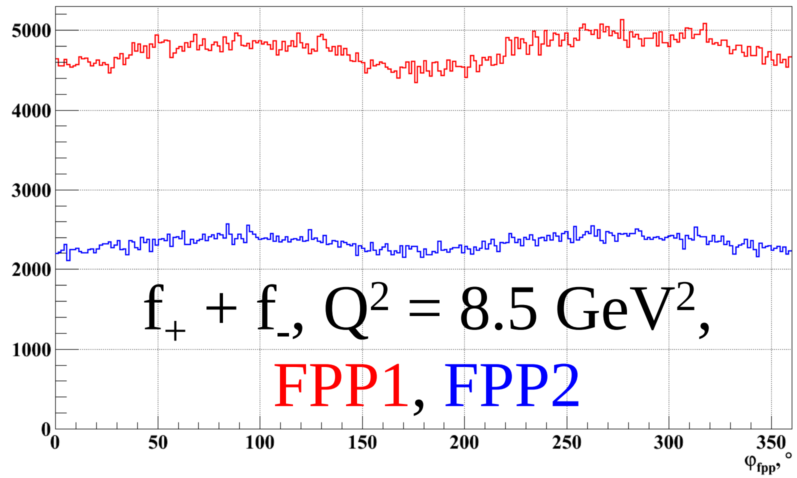

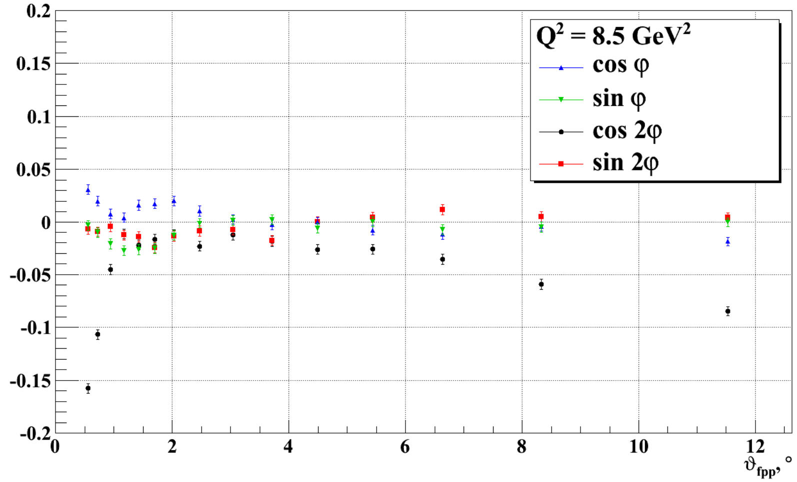

Polarized Target Asymmetry and G_E^n

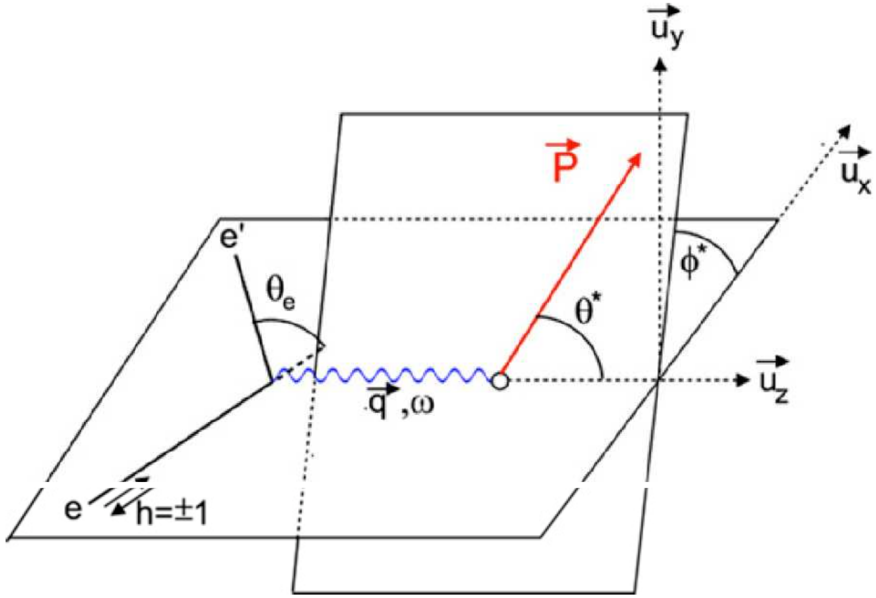

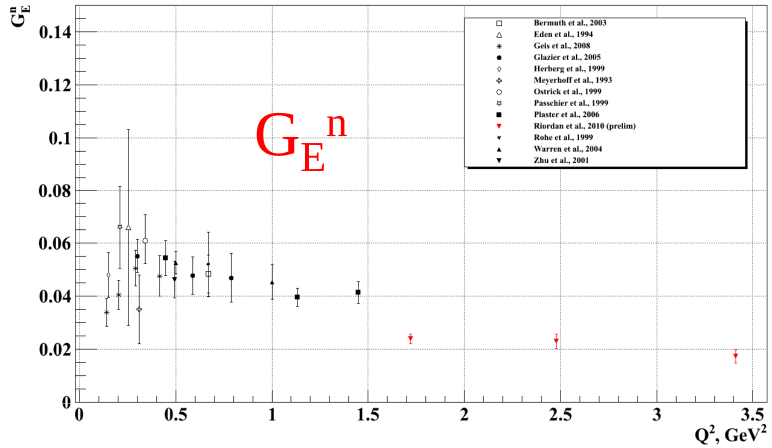

$$A_{phys} = -\frac{2\sqrt{\tau(1+\tau)}\tan\frac{\theta_e}{2}}{\frac{G_E^2}{G_M^2}+\frac{\tau}{\epsilon}}\left[\sin\theta^*\cos\phi^*\frac{G_E}{G_M} + \sqrt{\tau\left[1+(1+\tau)\tan^2\frac{\theta_e}{2}\right]}\cos\theta^*\right]$$

- Polarized beam on polarized target
- Beam helicity asymmetry sensitive to G_E/G_M
- Maximal sensitivity for target polarization perp. to q in scattering plane
- Nearly all G_E^n data obtained from:

$$^3\overrightarrow{He}(\vec{e},e'n),\ ^3\overrightarrow{He}(\vec{e},e'),\ ^2H(\vec{e},e'\vec{n})$$

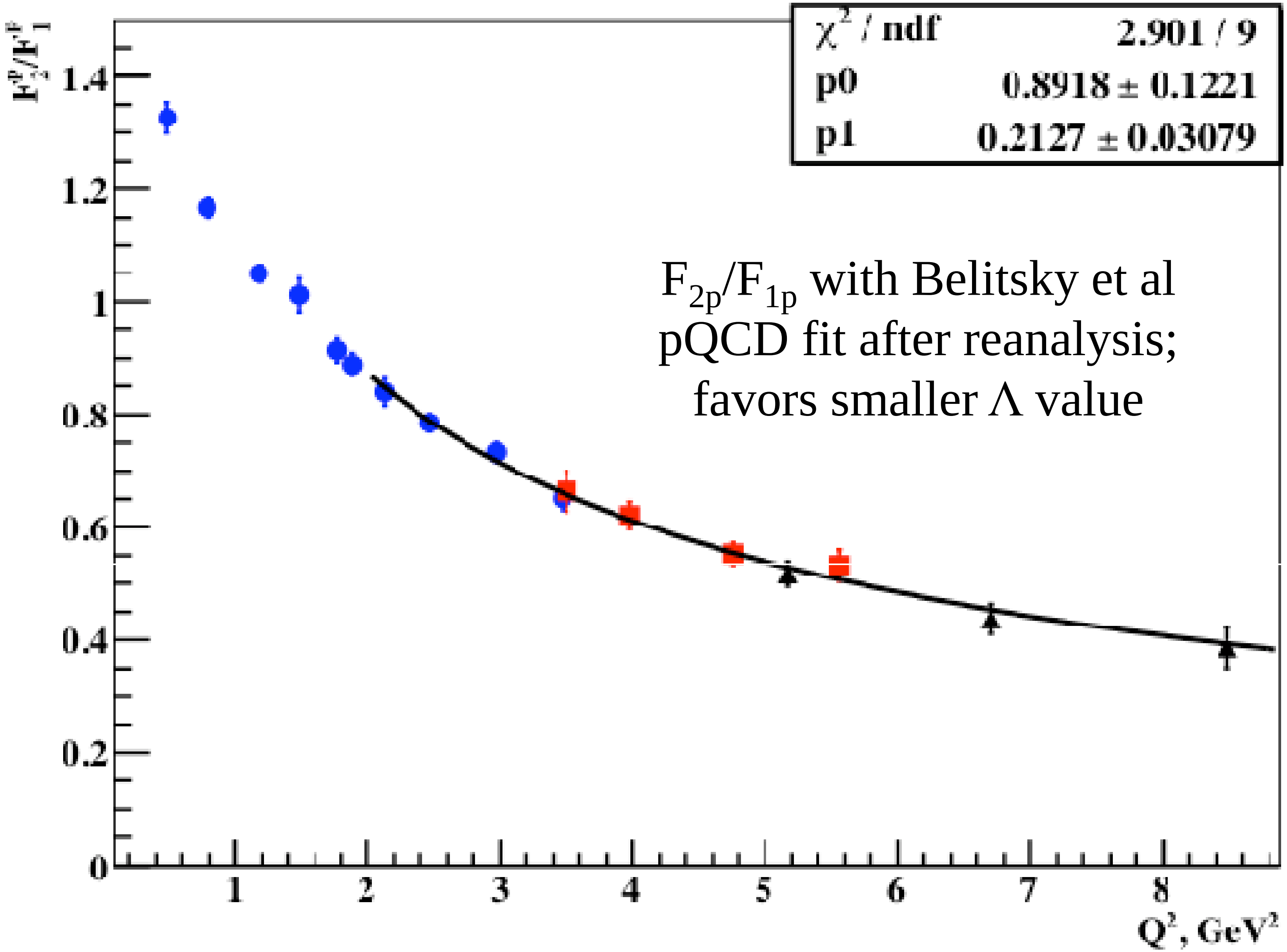

F_{2p}/F_{1p} with Belitsky et al pQCD fit after reanalysis; favors smaller Λ value

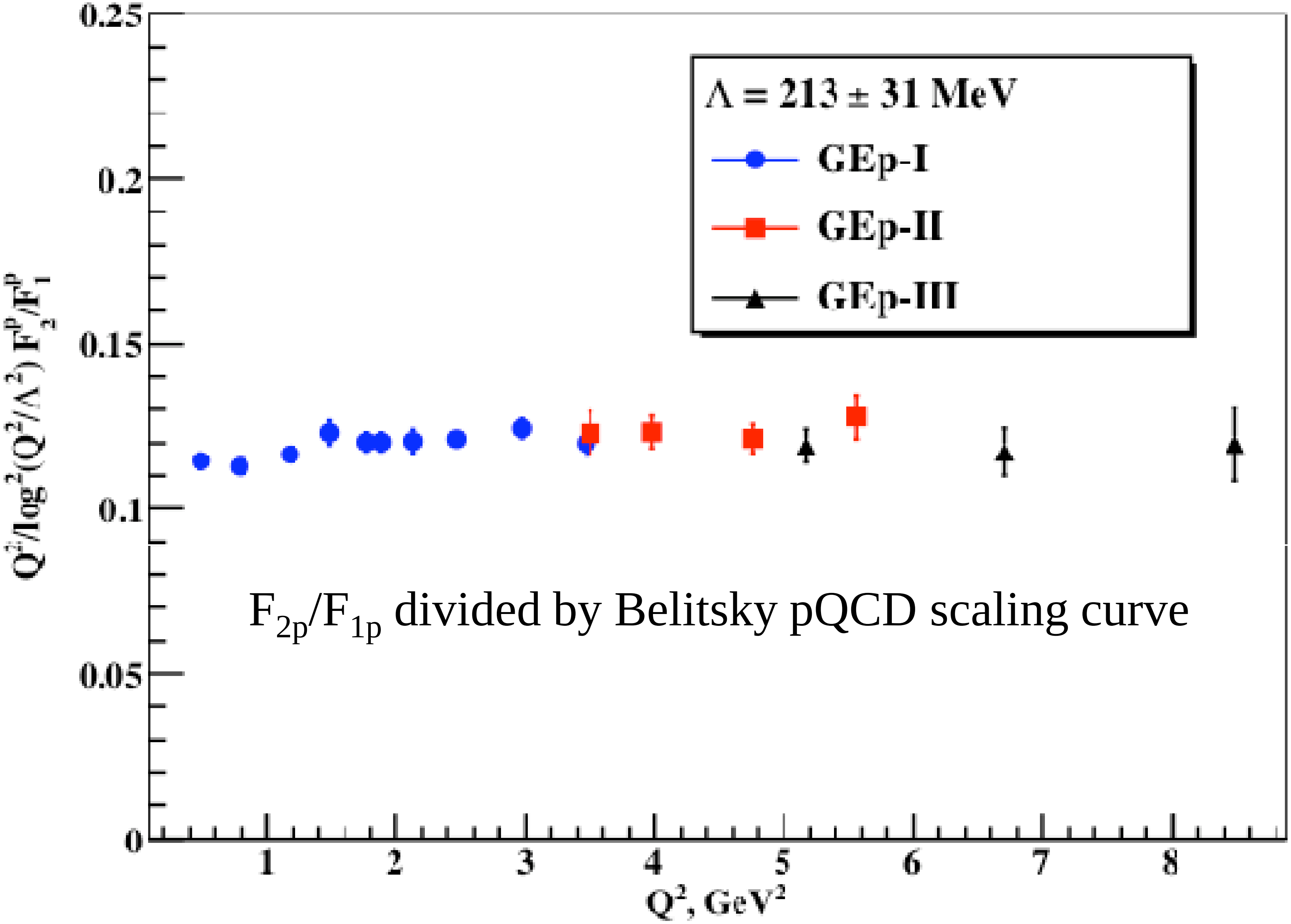
Λ = 213 ± 31 MeV
GEp-I
GEp-II
GEp-III
$Q^2/\log^2(Q^2/\Lambda^2)\, F_2^p/F_1^p$
Q^2, GeV^2
0.25
0.2
0.15
0.1
0.05
0
1
2
3
4
5
6
7
8
F_{2p}/F_{1p} divided by Belitsky pQCD scaling curve

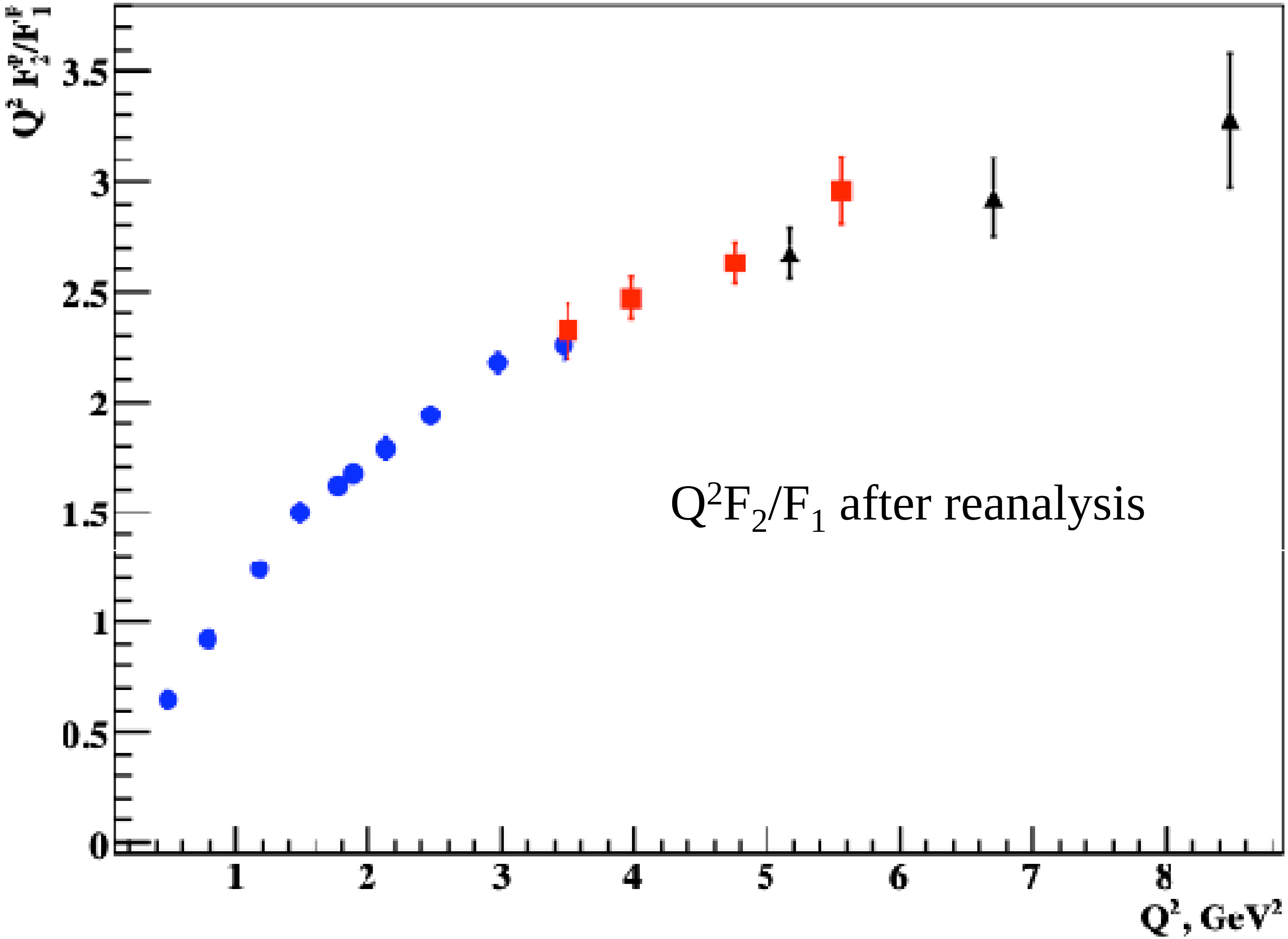
$Q^2 F_2^p/F_1^p$
3.5
3
2.5
2
1.5
1
0.5
0
1
2
3
4
5
6
7
8
Q^2, GeV^2
Q^2F_2/F_1 after reanalysis

Elastic Event Selection

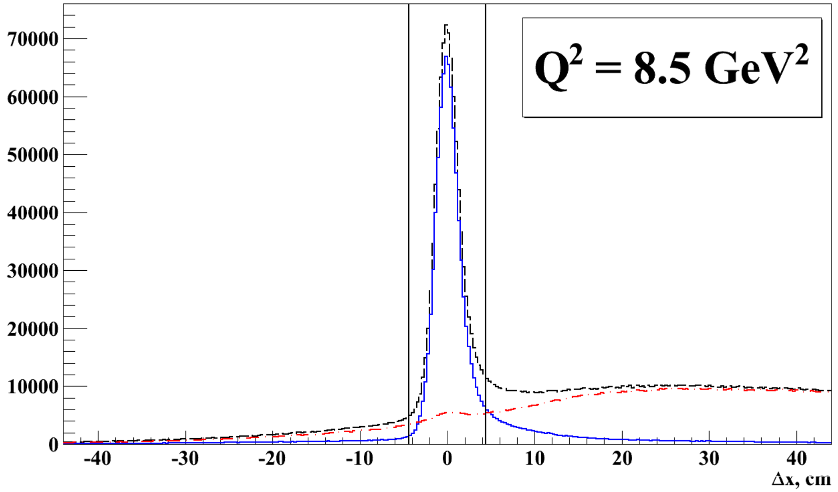

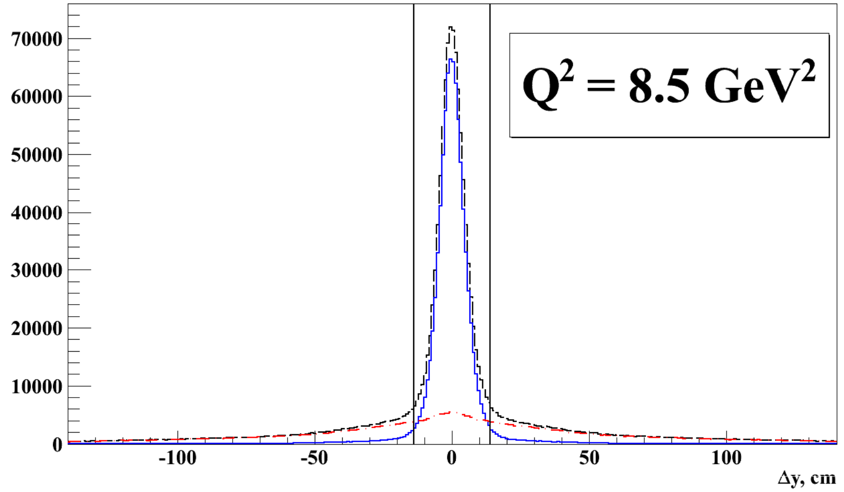

- Electron coordinates/angles + proton momentum measured with excellent resolution; use these quantities to define cut variables
- Calculate θ_e from E_e, p_p
- Calculate φ_e from φ_p (coplanarity)
- Project from vertex to BigCal, compare to measured electron coordinates
- Above: projections of horizontal (dx) and vertical (dy) coordinate differences:
  - **No cut, 3σ dp cut, 3σ dp anticut**
  - Tight dp cut rejects some small fraction of elastic events (small "bumps")

Traditional interpretation: Charge and Magnetization Densities

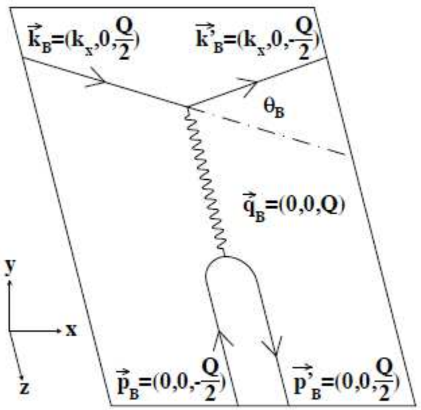

Figure 1 2: Elastic scattering in the Breit frame

$$\widetilde{\rho}_{ch}(k) = G_E(Q^2)(1+\tau)^{\lambda_E},$$

$$\mu\widetilde{\rho}_m(k) = G_M(Q^2)(1+\tau)^{\lambda_M},$$

$$\rho(r) = \frac{2}{\pi}\int_0^\infty dk\, k^2 j_0(kr)\widetilde{\rho}(k).$$

$$k^2 = \frac{Q^2}{1+\tau}$$

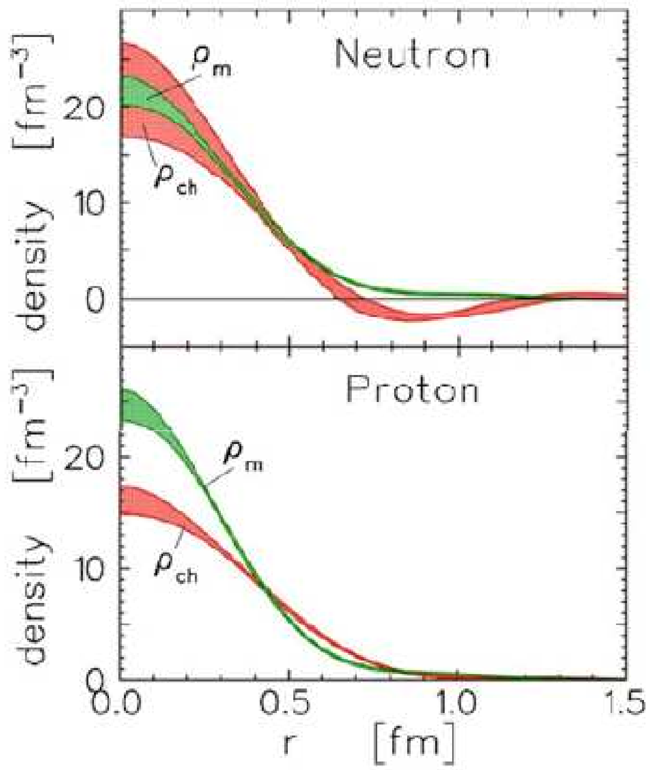

$$\rho_{ch}^{NR}(r) = \frac{2}{\pi}\int_0^\infty dQ\, Q^2 j_0(Qr) G_E(Q^2),$$

$$\mu\rho_m^{NR}(r) = \frac{2}{\pi}\int_0^\infty dQ\, Q^2 j_0(Qr) G_M(Q^2),$$

J. J. Kelly: PRC 66, 065203 (2002)